17. Hodgkin AL, Huxley AF. A quantitative description of membrane current and its application to conduction and excitation in nerve. *J Physiol* 1952; **117:** 500–544.
18. Newton-Cheh C, Guo CY, Larson MG, Musone SL, Surti A, Camargo AL, et al. Common genetic variant in KCNH2 is associated with QT interval duration: The Framingham Heart Study. *Circulation* 2007; **116:** 1128–1136.
19. Plant LD, Bowers PN, Liu Q, Morgan T, Zhang T, State MW, et al. A common cardiac sodium channel variant associated with sudden infant death in African Americans, SCN5A S1103Y. *J Clin Invest* 2006; **116:** 430–435.
20. Nishio Y, Makiyama T, Itoh H, Sakaguchi T, Ohno S, Gong YZ, et al. D85N, a KCNE1 polymorphism, is a disease-causing gene variant in long QT syndrome. *J Am Coll Cardiol* 2009; **54:** 812–819.
21. Newton-Cheh C, Eijgelsheim M, Rice KM, de Bakker PI, Yin X, Estrada K, et al. Common variants at ten loci influence QT interval duration in the QTGEN study. *Nat Genet* 2009; **41:** 399–406.
22. Pfeufer A, Sanna S, Arking DE, Müller M, Gateva V, Fuchsberger C, et al. Common variants at ten loci modulate the QT interval duration in the QTSCD study. *Nat Genet* 2009; **41:** 407–414.
23. Arking DE, Pfeufer A, Post W, Kao WH, Newton-Cheh C, Ikeda M, et al. A common genetic variant in the NOS1 regulator NOS1AP modulate cardiac repolarization. *Nat Genet* 2006; **38:** 644–651.
24. Crotti L, Monti MC, Insolia R, Peljto A, Goosen A, Brink PA, et al. NOS1AP is a genetic modifier of the long-QT syndrome. *Circulation* 2009; **120:** 1657–1663.
25. Sakaguchi T, Shimizu W, Itoh H, Noda T, Miyamoto Y, Nagaoka I, et al. Hydroxyzine, a first generation H(1)-receptor antagonist, inhibits human ether-a-go-go-related gene (HERG) current and causes syncope in a patient with the HERG mutation. *J Pharmacol Sci* 2008; **108:** 462–471.
26. Lupoglazoff JM, Cheav T, Baroudi G, Berthet M, Denjoy I, Cauchemez B, et al. Homozygous SCN5A mutation in long-QT syndrome with functional two-to-one atrioventricular block. *Circ Res* 2001; **89:** E16–E21.
27. Chang CC, Acharfi S, Wu MH, Chiang FT, Wang JK, Sung TC, et al. A novel SCN5A mutation manifests as a malignant form of long QT syndrome with perinatal onset of tachycardia/bradycardia. *Cardiovasc Res* 2004; **64:** 268–278.
28. Miura M, Yamagishi H, Morikawa Y, Matsuoka R. Congenital long QT syndrome and 2:1 atrioventricular block with a mutation of the SCN5A gene. *Pediatr Cardiol* 2003; **24:** 70–72.
29. Nakamura H, Kurokawa J, Bai CX, Asada K, Xu J, Oren RV, et al. Progesterone regulates cardiac repolarization through a nongenomic pathway: An in vitro patch-clamp and computational modeling study. *Circulation* 2007; **116:** 2913–2922.
30. Makkar RR, Fromm BS, Steinman RT, Meissner MD, Lehmann MH. Female gender as a risk factor for torsades de pointes associated with cardiovascular drugs. *JAMA* 1993; **270:** 2590–2597.
31. Locati EH, Zareba W, Moss AJ, Schwartz PJ, Vincent GM, Lehmann MH, et al. Age- and sex-related differences in clinical manifestations in patients with congenital long-QT syndrome: Findings from the International LQTS Registry. *Circulation* 1998; **97:** 2237–2244.

KCNE2 modulation of Kv4.3 current and its potential role in fatal rhythm disorders

Jie Wu, PhD,* Wataru Shimizu, MD, PhD,† Wei-Guang Ding, MD, PhD,‡ Seiko Ohno, MD, PhD,§ Futoshi Toyoda, PhD,‡ Hideki Itoh, MD, PhD,¶ Wei-Jin Zang, MD, PhD,* Yoshihiro Miyamoto, MD, PhD,‖ Shiro Kamakura, MD, PhD,† Hiroshi Matsuura, MD, PhD,‡ Koonlawee Nademanee, MD, FACC,# Josep Brugada, MD,** Pedro Brugada, MD,†† Ramon Brugada, MD, PhD, FACC,‡‡ Matteo Vatta, PhD,§§¶¶ Jeffrey A. Towbin, MD, FAAP, FACC,§§ Charles Antzelevitch, PhD, FACC, FAHA, FHRS,‖‖ Minoru Horie, MD, PhD¶

*From the *Pharmacology Department, Medical School of Xi'an Jiaotong University. Xi'an, Shaanxi, China, †Division of Cardiology, Department of Internal Medicine, National Cardiovascular Center, Suita, Japan, ‡Department of Physiology, Shiga University of Medical Science, Ohtsu, Japan, §Department of Cardiovascular Medicine, Kyoto University of Graduate School of Medicine, Kyoto, Japan, ¶Department of Cardiovascular Medicine, Shiga University of Medical Science, Shiga, Japan, ‖Laboratory of Molecular Genetics, National Cardiovascular Center, Suita, Japan, #Department of Medicine (Cardiology), University of Southern California, Los Angeles, California, **Cardiovascular Institute, Hospital Clinic, University of Barcelona, Barcelona, Spain, ††Heart Rhythm Management Centre, Free University of Brussels (UZ Brussel) VUB, Brussels, Belgium, ‡‡School of Medicine, Cardiovascular Genetics Center, University of Girona, Girona, Spain, §§Departments of Pediatrics, Baylor College of Medicine, Houston, Texas, ¶¶Department of Molecular Physiology and Biophysics, Baylor College of Medicine, Houston, Texas, and ‖‖Masonic Medical Research Laboratory, Utica, New York.*

BACKGROUND The transient outward current I_{to} is of critical importance in regulating myocardial electrical properties during the very early phase of the action potential. The auxiliary β subunit *KCNE2* recently was shown to modulate I_{to}.

OBJECTIVE The purpose of this study was to examine the contributions of *KCNE2* and its two published variants (M54T, I57T) to I_{to}.

METHODS The functional interaction between Kv4.3 (α subunit of human I_{to}) and wild-type (WT), M54T, and I57T *KCNE2*, expressed in a heterologous cell line, was studied using patch-clamp techniques.

RESULTS Compared to expression of Kv4.3 alone, co-expression of WT *KCNE2* significantly reduced peak current density, slowed the rate of inactivation, and caused a positive shift of voltage dependence of steady-state inactivation curve. These modifications rendered Kv4.3 channels more similar to native cardiac I_{to}. Both M54T and I57T variants significantly increased I_{to} current density and slowed the inactivation rate compared with WT *KCNE2*. Moreover, both variants accelerated the recovery from inactivation.

CONCLUSION The study results suggest that *KCNE2* plays a critical role in the normal function of the native I_{to} channel complex in human heart and that M54T and I57T variants lead to a gain of function of I_{to}, which may contribute to generating potential arrhythmogeneity and pathogenesis for inherited fatal rhythm disorders.

KEYWORDS Cardiac arrhythmia; M54T variation; I57T variation; *KCNE2*; Kv4.3; Sudden cardiac death

ABBREVIATIONS CHO = Chinese hamster ovary; **HERG** = human ether-a-go-go related gene; **WT** = wild type

Introduction

Classic voltage-gated K^+ channels consist of four pore-forming (α) subunits that contain the voltage sensor and ion selectivity filter[1,2] and accessory regulating (β) subunits.[3] *KCNE* family genes encode several kinds of β subunits consisting of single transmembrane-domain peptides that co-assemble with α subunits to modulate ion selectivity, gating kinetics, second messenger regulation, and the pharmacology of K^+ channels. Association of the *KCNE1* product minK with the α subunit Kv7.1 encoding *KCNQ1* forms the slowly activating delayed rectifier K^+ current I_{Ks} in the heart.[4,5] In contrast, association of the *KCNE2* product MiRP1 with the human ether-a-go-go related gene (HERG) forms the cardiac rapid delayed rectifier K^+ current I_{Kr}.[6]

The first two authors contributed equally to the original concept and the authorship of this study. This study was supported by grants from the Ministry of Education, Culture, Sports, Science, Technology Leading Project for Biosimulation to Dr. Horie; Health Sciences Research grants (H18-Research on Human Genome-002) from the Ministry of Health, Labour and Welfare, Japan to Drs. Shimizu and Horie; the National Natural Science Foundation of China (Key Program, No.30930105; General Program, No. 30873058, 30770785) and the National Basic Research Program of China (973 Program, No. 2007CB512005) and CMB Distinguished Professorships Award (No. F510000/G16916404) to Dr. Zang; and National Institutes of Health Grant HL47678 and Free and Accepted Masons of New York State and Florida to Dr. Antzelevitch. **Address reprint requests and correspondence:** Dr. Minoru Horie, Department of Cardiovascular and Respiratory Medicine, Shiga University of Medical Science, Otsu, Shiga 520-2192, Japan. E-mail address: horie@belle.shiga-med.ac.jp. (Received August 20, 2009; accepted October 7, 2009.)

1547-5271/$ -see front matter doi:10.1016/j.hrthm.2009.10.012

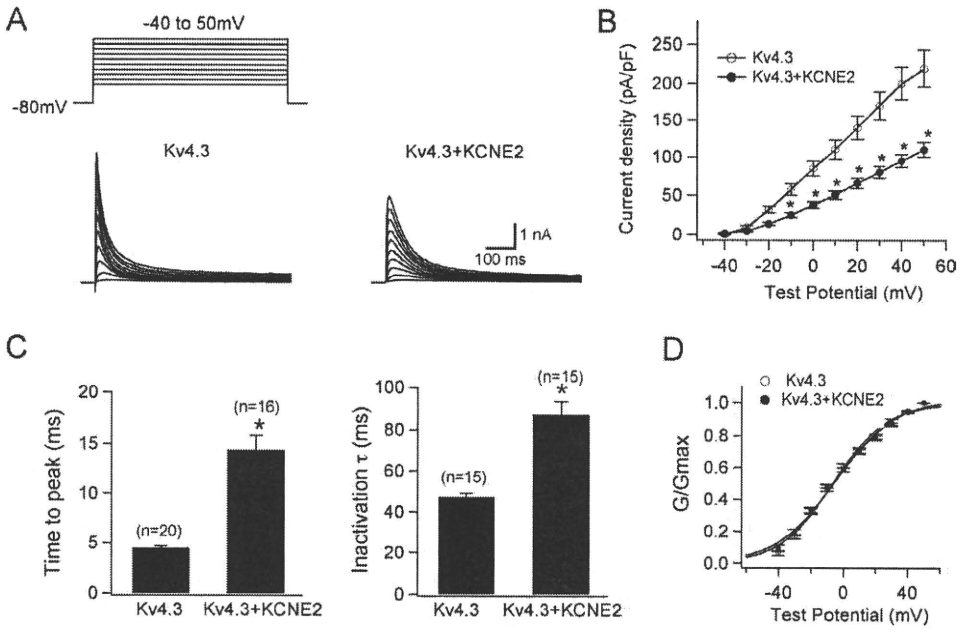

Figure 1 *KCNE2* co-expression with Kv4.3 produces smaller I_{to}-like currents with slower activation/inactivation kinetics. **A:** Representative current traces recorded from Chinese hamster ovary (CHO) cells expressing Kv4.3 **(left)** and Kv4.3 + *KCNE2* **(right).** As shown in the **inset** in panel A, depolarizing step pulses of 1-second duration were introduced from a holding potential of −80 mV to potentials ranging from −40 to +50 mV in 10-mV increments. **B:** Current–voltage relationship curve showing peak current densities in the absence and presence of co-transfected *KCNE2* (*P <.05 vs Kv4.3). **C:** Bar graphs showing the kinetic properties of reconstituted channel currents: time to peak of activation course **(left)** and inactivation time constants **(right)** measured using test potential to +20 mV (*P <.05 vs Kv4.3). Numbers in parentheses indicate numbers of experiments. **D:** Normalized conductance–voltage relationship for peak outward current of Kv4.3 and Kv4.3 + *KCNE2* channels.

Abbott et al reported that three *KCNE2* variants (Q9E, M54T, I57T) caused a loss of function in I_{Kr} and thereby were associated with the congenital or drug-induced long QT syndrome.[6,7] However, the reported QTc values in two index patients with M54T and I57T variants, both located in the transmembrane segment of MiRP1, were only mildly prolonged (390–500 ms and 470 ms).[6] We recently identified the same missense *KCNE2* variant, I57T, in which isoleucine was replaced by threonine at codon 57, in three unrelated probands showing a Brugada type 1 ECG. These findings are difficult to explain on the basis of a loss of function in I_{Kr}, thus leading us to explore other mechanisms.

Recent studies have demonstrated that interaction between α and β subunits (*KCNE*s) of voltage-gated K^+ channel is more promiscuous; for example, MiRP1 has been shown to interact with Kv7.1,[8–10] HCN1,[11] Kv2.1,[12] and Kv4.2.[13] These studies suggest that MiRP1 may also co-associate with Kv4.3 and contribute to the function of transient outward current (I_{to}) channels.[14] Indeed, a recent study reported that I_{to} is diminished in *kcne2* (–/–) mice.[15]

In the human heart, I_{to} currents are of critical importance in regulating myocardial electrical properties during the very early phase of the action potential and are thought to be central to the pathogenesis of Brugada-type ECG manifestations.[16] Antzelevitch et al demonstrated that a gain of function in I_{to} secondary to a mutation in *KCNE3* contributes to a Brugada phenotype by interacting with Kv4.3 and thereby promoting arrhythmogenicity.[14]

We hypothesized that mutations in *KCNE2* may have similar actions and characterize the functional consequences of interaction of wild-type (WT) and two mutant (I57T, M54T) MiRP1 with Kv4.3[17,18] using heterologous co-expression of these α and β subunits in Chinese hamster ovary (CHO) cells.

Methods

Heterologous expression of hKv4.3 and β subunits in CHO cells

Full-length cDNA fragment of *KCNE2* in pCR3.1 vector[10] was subcloned into pIRES-CD8 vector. This expression vector is useful in cell selection for later electrophysiologic study (see below). Two *KCNE2* mutants (M54T, I57T) were constructed using a Quick Change II XL site-directed mutagenesis kit according to the manufacturer's instructions (Stratagene, La Jolla, CA, USA) and subcloned to the same vector. Two *KCNE2* mutants were fully sequenced (ABI3100x, Applied Biosystems, Foster City, CA, USA) to ensure fidelity. Full-length cDNA encoding the short isoform of human Kv4.3 subcloned into the pIRES-GFP (Clontech, Palo Alto, CA, USA) expression vector was kindly provided by Dr. G.F. Tomaselli (Johns Hopkins University). Full-length cDNA encoding Kv channel-interacting protein (*KCNIP2*) subcloned into the PCMV-IRS expression vector was a kind gift from Dr. G.-N. Tseng (Virginia Commonwealth University). *KCND3* was transiently transfected into CHO cells together with *KCNE2* (or M54T or I57T) cDNA at equimolar ratio (*KCND3* 1.5 μg,

Table 1 Effects of *KCNE2* on Kv4.3 and Kv4.3 + KChIP2b

Parameter	Kv4.3	Kv4.3 *KCNE2*	Kv4.3 KChIP2b	Kv4.3 KChIP2b *KCNE2*
Current density at +20 mV (pA/pF)	142.0 ± 16.0 (n = 12)	66.0 ± 6.6* (n = 12)	191.5 ± 33.8 (n = 15)	77.8 ± 5.9† (n = 20)
Steady-state activation ($V_{0.5}$ in mV)	−6.5 ± 2.1 (n = 9)	−5.5 ± 1.7 (n = 11)	−7.5 ± 1.7 (n = 8)	−7.4 ± 1.4 (n = 8)
Steady-state inactivation ($V_{0.5}$ in mV)	−46.0 ± 1.3 (n = 10)	−40.8 ± 1.7* (n = 8)	−49.8 ± 1.4 (n = 7)	−44.5 ± 1.9† (n = 7)
τ of inactivation at +20 mV (τ_{inact} in ms)	47.3 ± 2.0 (n = 15)	87.2 ± 6.2* (n = 15)	47.5 ± 2.2 (n = 15)	66.6 ± 3.5† (n = 15)
Time to peak at +50 mV (TtP in ms)	4.5 ± 0.2 (n = 20)	14.4 ± 1.4* (n = 16)	4.1 ± 0.2 (n = 15)	6.1 ± 0.5† (n = 21)
τ of recovery from inactivation (ms)	419.6 ± 18.8 (n = 6)	485.6 ± 74.8 (n = 6)	89.2 ± 5.3 (n = 6)	60.2 ± 6.9† (n = 6)

*Significantly different from Kv4.3.
†Significantly different from Kv4.3 + KChIP2b.

KCNE2 1.5 μg) using Lipofectamine (Invitrogen Life Technologies, Carlsbad, CA, USA) according to the manufacturer's instructions. In one set of experiments, we also co-transfected equimolar levels of KChIP2b (*KCND3* 1.5 μg, *KCNE2* 1.5 μg, *KCNIP2* 1.5 μg). The transfected cells were then cultured in Ham's F-12 medium (Nakalai Tesque, Inc., Kyoto, Japan) supplemented with 10% fetal bovine serum (JRH Biosciences, Inc., Lenexa, KS, USA) and antibiotics (100 international units per milliliter penicillin and 100 μg/mL streptomycin) in a humidified incubator gassed with 5% CO_2 and 95% air at 37°C. The cultures were passaged every 4 to 5 days using a brief trypsin-EDTA treatment. The trypsin-EDTA treated cells were seeded onto glass coverslips in a Petri dish for later patch-clamp experiments.

Electrophysiologic recordings and data analysis

After 48 hours of transfection, a coverslip with cells was transferred to a 0.5-mL bath chamber at 25°C on an inverted microscope stage and perfused at 1 to 2 mL/min with extracellular solution containing the following (in mM): 140 NaCl, 5.4 KCl, 1.8 $CaCl_2$, 0.5 $MgCl_2$, 0.33 NaH_2PO_4, 5.5 glucose, and 5.0 HEPES; pH 7.4 with NaOH. Cells that emitted green fluorescence were chosen for patch-clamp experiments. If co-expressed with *KCNE2* (or its mutants), the cells were incubated with polystyrene microbeads precoated with anti-CD8 antibody (Dynabeads M450, Dynal, Norway) for 15 minutes. In these cases, cells that emitted green fluorescence and had attached beads were chosen for electrophysiologic recording. Whole-cell membrane currents were recorded with an EPC-8 patch-clamp amplifier (HEKA, Lambrecht, Germany), and data were low-pass filtered at 1 kHz, acquired at 5 kHz through an LIH-1600 analog-to-digital converter (HEKA), and stored on hard disk using PulseFit software (HEKA). Patch pipettes were fabricated from borosilicate glass capillaries (Narishige, Tokyo, Japan) using a horizontal microelectrode puller (P-97, Sutter Instruments, Novato, CA, USA) and the pipette tips fire-polished using a microforge. Patch pipettes had a resistance of 2.5 to 5.0 MΩ when filled with the following pipette solution (in mM): 70 potassium aspartate, 50 KCl, 10 KH_2PO_4, 1 $MgSO_4$, 3 Na_2-ATP (Sigma, Japan, Tokyo), 0.1 Li_2-GTP (Roche Diagnostics GmbH, Mannheim, Germany), 5 EGTA, and 5 HEPES (pH 7.2).

Cell membrane capacitance (C_m) was calculated from 5 mV-hyperpolarizing and depolarizing steps (20 ms) applied from a holding potential of −80 mV according to Equation 1[19]:

$$C_m = \tau_c I_0/\Delta V_m(1 - I_\infty/I_0), \quad (1)$$

where τ_c = time constant of capacitance current relaxation, I_0 = initial peak current amplitude, ΔV_m = amplitude of voltage step, and I_∞ = steady-state current value. Whole-cell currents were elicited by a family of depolarizing voltage steps from a holding potential of −80 mV. The difference between the peak current amplitude and the current at the end of a test pulse (1-second duration) was referred to as the transient outward current. To control for cell size variability, currents were expressed as densities (pA/pF).

Steady-state activation curves were obtained by plotting the normalized conductance as a function of peak outward potentials. Steady-state inactivation curves were generated by a standard two-pulse protocol with a conditioning pulse of 500-ms duration and obtained by plotting the normalized current as a function of the test potential. Steady-state inactivation/activation kinetics were fitted to the following Boltzmann equation (Eq. 2):

$$Y(V) = 1/(1 + \exp[(V_{1/2} - V)/k]), \quad (2)$$

where Y = normalized conductance or current, $V_{1/2}$ = potential for half-maximal inactivation or activation, respectively, and k = slope factor.

Data relative to inactivation time constants, time to peak, and mean current levels were obtained by using current data recorded at +50 mV or +20 mV. Recovery from inactivation was assessed by a standard paired-pulse protocol: a 400-ms test pulse to +50 mV (P1) followed by a variable

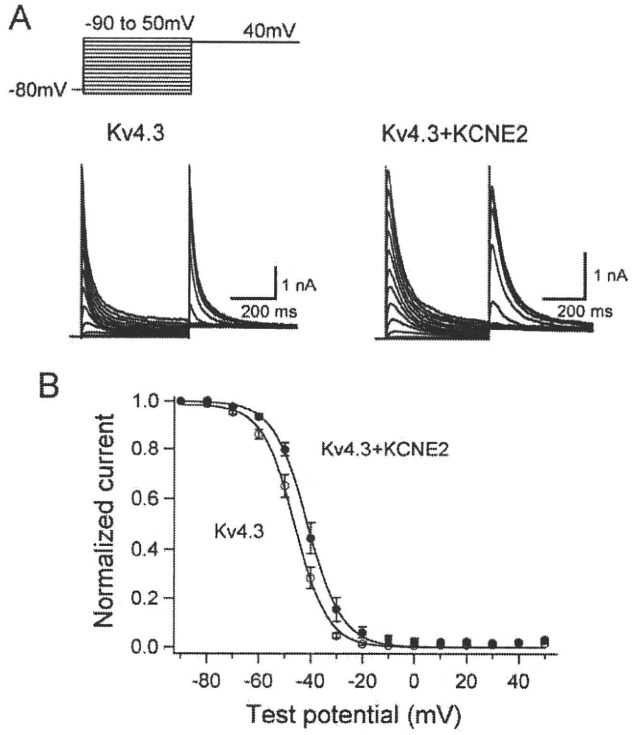

Figure 2 *KCNE2* co-expression with Kv4.3 causes a positive shift of voltage dependence of steady-state inactivation. **A:** Representative Kv4.3 and Kv4.3 + *KCNE2* current traces induced by 500-ms pulses (P1) from −90 to +50 mV applied from the holding potential −80 mV in 10-mV steps followed by a second pulse (P2) to +40 mV. **B:** Steady-state inactivation curves for Kv4.3 *(open circles)* and Kv4.3 + *KCNE2 (closed circles)* channels.

recovery interval at −80 mV and then a second test pulse to +50 mV (P2). Both the inactivation time constants and the time constant for recovery from inactivation were determined by fitting the data to a single exponential (Eq. 3):

$$I(t) \text{ (or P2/P1)} = A + B_{exp}(-t/\tau), \quad (3)$$

where I(t) = current amplitude at time t, A and B = constants, and τ = inactivation time constant or time constant for recovery from inactivation. For measurement of recovery from inactivation, the plot of P2/P1 instead of I(t) was used.

All data were given as mean ± SEM. Statistical comparisons between two groups were analyzed using Student's unpaired t-test. Comparisons among multiple groups were analyzed using analysis of variance followed by Dunnett test. $P < .05$ was considered significant.

Results

Effects of *KCNE2* on Kv4.3 currents and its gating kinetics

WT *KCNE2* initially was co-expressed with *KCND3*, the gene encoding Kv4.3, the α subunit of the I_{to} channel,[17,18] in CHO cells. Figure 1A shows representative whole-cell current traces recorded from cells transfected with *KCND3* and co-transfected with (right) or without (left) *KCNE2*. Cells expressing Kv4.3 channels alone showed rapidly activating and inactivating currents. Co-expression of *KCNE2* significantly reduced peak current densities as summarized in the current–voltage relationship curve shown in Figure 1B and slowed both activation and inactivation kinetics (Table 1). Figure 1C (left) shows mean time intervals from the onset of the pulse to maximum current (time to peak), whereas the right panel shows time constants of inactivation (at +20 mV) obtained using Equation 3. Thus, co-transfection of *KCNE2* significantly increased both the time to peak and the time constant.

In contrast, *KCNE2* did not affect the voltage dependence of steady-state activation as assessed by plotting the normalized conductance as a function of test potential (Figure 1D). Fitting to the Boltzmann equation (Eq. 2) yielded half-maximal activation potentials of −6.5 ± 2.1 mV for Kv4.3 alone (open circles) and −5.5 ± 1.7 mV for Kv4.3 + *KCNE2* channels (filled circles, P = NS; Table 1). These findings are consistent with those previously reported for studies using *Xenopus* oocytes, CHO cells, and HEK293 cells.[20,21]

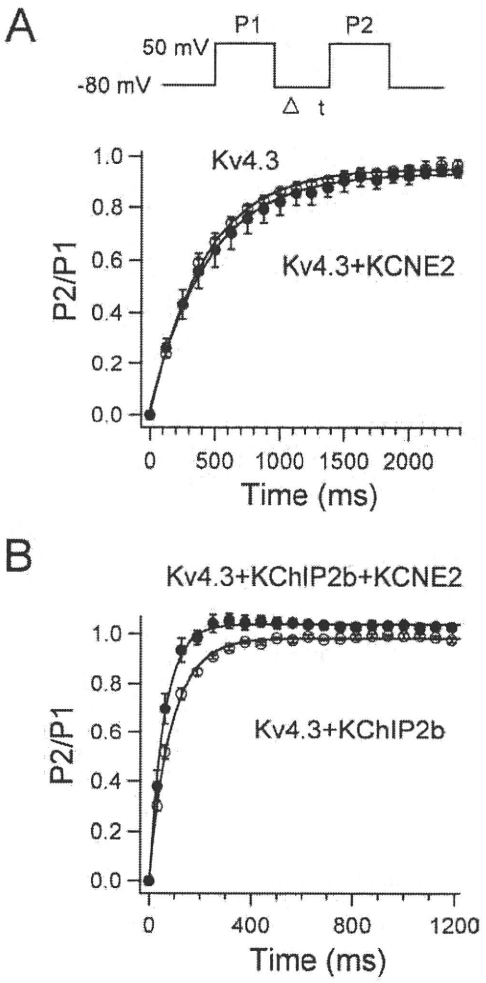

Figure 3 Effects of *KCNE2* co-expression on recovery from inactivation of Kv4.3 **(A)** and Kv4.3 + KChIP2b **(B)** currents. Recovery from inactivation was assessed by a two-pulse protocol **(A, inset):** a 400-ms test pulse to +50 mV (P1) followed by a variable interval at −80 mV, then by a second test pulse to +50 mV (P2). Data were fit to a single exponential.

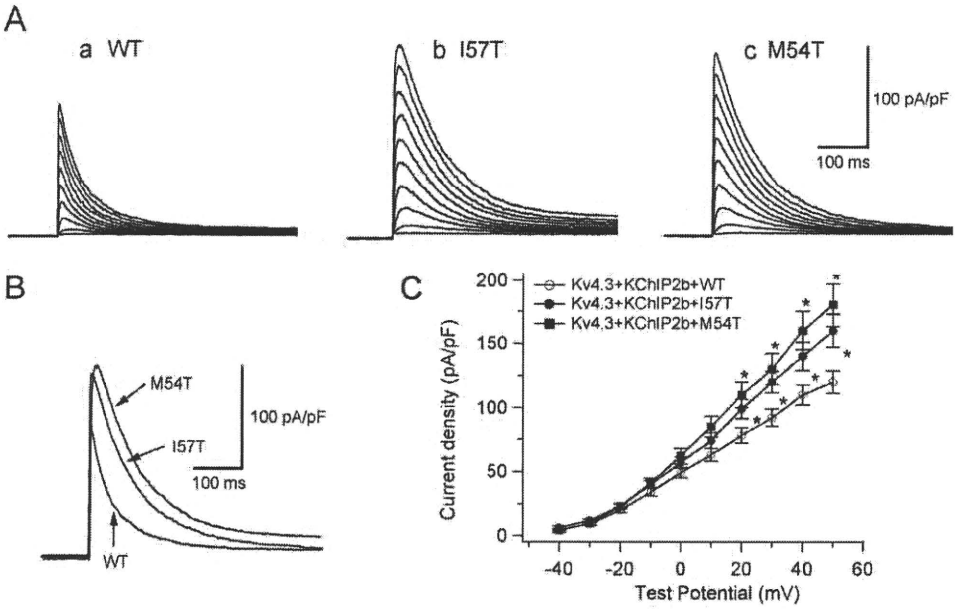

Figure 4 Two *KCNE2* transmembrane variants, I57T and M54T, increase the reconstituted Kv4.3 + KChIP2b channel current and slow its inactivation. **A:** Three sets of current traces elicited by depolarizing pulses for 500 ms from a holding potential of −80 mV to potentials ranging between −40 and +50 mV in 10-mV increments (same protocol as in experiments of Figure 1A). **B:** Superimposition of three original current traces recorded upon depolarization showing variant-related increase in peak outward current density. **C:** Current–voltage relationship curve showing average peak outward current densities (*P <.05 vs Kv4.3 + KChIP2b + WT). WT = wild type.

KCNE2 co-expression also caused a positive shift (approximately +5 mV) of voltage dependence of steady-state inactivation. Steady-state inactivation was assessed using a double-step pulse method (Figure 2A, inset). Peak outward currents recorded at various levels of prepulse (Figure 2A) were normalized by that measured after a 500-ms prepulse at −90 mV and are plotted as a function of prepulse test potentials (Figure 2B). Half-inactivation potentials of steady-state inactivation, determined by fitting data to the Boltzmann equation (Eq. 2), were −46.0 ± 1.3 mV for Kv4.3 (open circles) and −40.8 ± 1.7 mV for Kv4.3 + *KCNE2* (filled circles, P <.01), consistent with the observation of Tseng's group.[13]

A double-pulse protocol (Figure 3A, inset) was used to test the effect of *KCNE2* co-expression on the time course for recovery from inactivation. Figure 3A shows the time course of recovery of Kv4.3 alone (open circles) and Kv4.3 + *KCNE2* (filled circles). Mean time constants for recovery from inactivation were not significantly different, indicating that co-transfection of *KCNE2* did not affect the time course of recovery from inactivation.

Effects of *KCNE2* on Kv4.3 + KChIP2b current and its gating kinetics

For human native cardiac I_{to}, KChIP2 has been shown to serve as a principal β subunit.[22–25] Accordingly, in another series of experiments, we examined the effect of WT and mutant *KCNE2* on Kv4.3 + KChIP2b current. Consistent with previous reports, in the presence of KChIP2, Kv4.3 currents showed a significantly faster recovery from inactivation (Figure 3B and Table 1).[26,27] Co-expression of WT *KCNE2* produced similar changes on Kv4.3 + KChIP2b current as on Kv4.3 current (Table 1). Kv4.3 + KChIP2b current recovery from inactivation was further accelerated: average time constant was 89.2 ± 6.5 ms for Kv4.3 + KChIP2b alone (open circles) and 60.2 ± 8.4 ms for Kv4.3 + KChIP2b + *KCNE2* (filled circles, P <.05). In 16 of 21 cells transfected with *KCNE2*, we observed an "overshoot" phenomenon, which is commonly seen during recording of native I_{to} in human ventricular myocytes.[28]

KCNE2 variants increase Kv4.3 + KChIP2b current and alter its gating kinetics

The I57T variant was first identified in an asymptomatic middle-aged woman with very mild QT prolongation.[6] In addition to this variant, the authors reported another *KCNE2* variant of the transmembrane segment (M54T) that was associated with ventricular fibrillation during exercise in a middle-aged woman. This patient appeared to show a wide range of QTc interval (390–500 ms). Therefore, we tested the functional effects of these two transmembrane *KCNE2* variants on Kv4.3 + KChIP2b currents.

The three panels of Figure 4A show three sets of current traces elicited by depolarizing pulses from a holding potential of −80 mV in cells co-transfected with WT (a), I57T (b), or M54T (c) *KCNE2*. Neither variant caused a significant shift of half-maximal activation voltage: −7.4 ± 1.4 mV (n = 8) for co-expression of WT *KCNE2*, −6.1 ± 1.5 mV (n = 8) for I57T, and −6.6 ± 1.6 mV (n = 8) for M54T. Both variants significantly increased I_{to} density: 125.0 ± 10.6 pA/pF in WT *KCNE2* (n = 21), 178.1 ± 12.1 pA/pF with I57T (n = 9), and 184.3 ± 27.9 pA/pF with M54T (n = 9, Figure 4C).

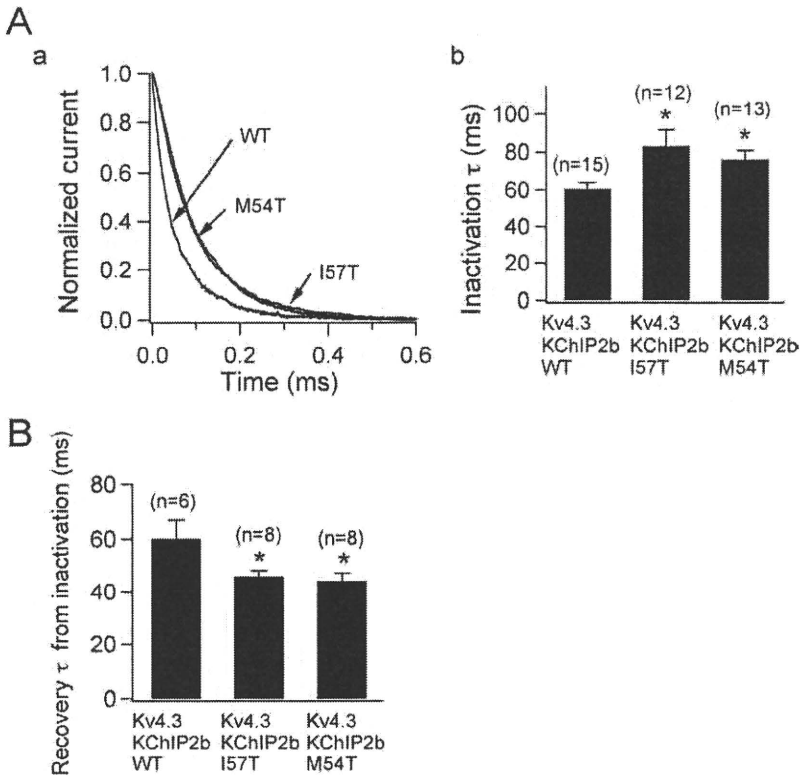

Figure 5 Two *KCNE2* variants slow inactivation kinetics and accelerate recovery from inactivation. **A, a:** Three current traces obtained from Chinese hamster ovary (CHO) cells transfected with wild-type (WT), I57T, and M54T *KCNE2* variant co-expressed with Kv4.3 and KChIP2b. Traces, which are normalized and superimposed, show that the variants slow inactivation. **A, b:** Time constants of decay at +20 mV for WT and variant *KCNE2* (*P <.05 vs Kv4.3 + KChIP2b + WT). Numbers in parentheses indicate numbers of observations. **B:** Time constants of recovery from inactivation recorded using a double-pulse protocol (*P <.05 vs Kv4.3 + KChIP2b + WT). Numbers in parentheses indicate numbers of observations.

Figure 5A shows the three traces depicted in Figure 4B normalized to their peak current level. This representation shows that the time course of inactivation of the two variant currents is slowed. The current decay was fitted by Equation 3 and the time constants (at +20 mV) summarized in Figure 5A, panel b. Finally, Figure 5B shows that the time constants of recovery of the two mutant channels from inactivation were significantly reduced. Thus, compared to WT *KCNE2*, recovery of reconstituted Kv4.3 + KChIP2b channels from inactivation was significantly accelerated with both I57T and M54T mutants.

Discussion

Kv4.3/KChIP2/MiRP1 complex can recapitulate the native I_{to}

In the present study, co-expression of WT *KCNE2* produced changes in kinetic properties (Figures 1–3 and Table 1) that led to close recapitulation of native cardiac I_{to}.[28,29] Notably, in addition to causing a positive shift of steady-state inactivation (Figure 2), *KCNE2* co-expression hastened the recovery of Kv4.3 + KChIP2b channels from inactivation (Figure 3). These modifications rendered Kv4.3 + KChIP2b channels more similar to native cardiac I_{to}, suggesting that *KCNE2* may be an important component of the native I_{to} channel complex. In contrast to a previous observation in HEK293 cells,[21] *KCNE2* co-expression decreased the current density of Kv4.3 and Kv4.3 + KChIP2b channel current in the present study, which seems to be a more reasonable result as the native I_{to} density reportedly was smaller in isolated human heart.[28] *KCNE2* co-expression has also been shown to reduce the density of Kv7.1[8,9] and HERG[6,7] channels.

Similar to the result of Deschenes and Tomaselli,[21] we failed to observe an overshoot during recovery from inactivation when *KCNE2* was co-expressed with Kv4.3 (Figure 3A), which is in contrast to the report of another group.[13] However, co-expression of *KCNE2* with Kv4.3 + KChIP2 channels produced an overshoot (Figure 3B), consistent with the report of Wettwer's group.[25] Wettwer et al also found that other *KCNE* subunits either were ineffective or induced only a small overshoot in CHO cells. Therefore, both MiRP1 and KChIP2 subunits are sufficient and necessary to recapitulate native I_{to} in the heart. Considering that the overshoot phenomenon has been described only in human ventricular I_{to} channels of the epicardial but not endocardial region,[28] these results may further implicate participation of MiRP1 and KChIP2 in the I_{to} channel complex in epicardium.

KCNE2 variants may alter the arrhythmogenic substrate by modulating I_{to}

Heterologous expression in CHO cells was conducted to examine the functional effects of I57T and M54T variants on Kv4.3 + KChIP2 channels. Both I57T and M54T

KCNE2 variants significantly (1) increased peak transient outward current density (Figure 4), (2) slowed the decay of the reconstituted I_{to} (Figure 5A), and (3) accelerated its recovery from inactivation (Figure 5B). Both variants thus caused an important gain of function in human I_{to}. These sequence changes may play a role in modulating I_{to} and thereby predispose to some inherited fatal rhythm disorders.

Functional effects on I_{to} induced by I57T and M54T resemble each other, increasing I_{to} density and accelerating its recovery from inactivation. The gain of function in I_{to} opposes the fast inward Na^+ currents during phase 0 of the action potential, leading to all or none repolarization at the end of phase 1 and loss of the epicardial action potential dome, thus promoting phase 2 reentry and fatal ventricular arrhythmias.[30]

Another *KCNE2* variant (M54T) associated with fatal arrhythmias was first identified in a woman who had a history of ventricular fibrillation and varied QT intervals.[6] It is possible that her arrhythmia was also related to a gain of function in I_{to} secondary to this variation in *KCNE2*. Interestingly, the I57T variant has been reported to produce a loss of function of HERG or Kv7.1 channels, thereby predisposing to long QT syndrome,[6,8] indicating that the same *KCNE2* variant could cause two different cardiac rhythm disorders, similar to long QT syndrome and Brugada syndrome caused by *SCN5A* mutations.[31,32]

References

1. Kass RS, Freeman LC. Potassium channels in the heart: cellular, molecular, and clinical implications. Trends Cardiovasc Med 1993;3:149–159.
2. MacKinnon R. Determination of the subunit stoichiometry of a voltage-activated potassium channel. Nature 1991;350:232–235.
3. Abbott GW, Goldstein SA. A superfamily of small potassium channel subunits: form and function of the MinK-related peptides (MiRPs). Q Rev Biophys 1998;31:357–398.
4. Barhanin J, Lesage F, Guillemare E, Fink M, Lazdunski M, Romey G. KvLQT1 and IsK (minK) proteins associate to form the I_{Ks} cardiac potassium current. Nature 1996;384:78–80.
5. Sanguinetti MC, Curran ME, Zou AR, et al. Coassembly of KvLQT1 and minK (I_{Ks}) proteins to form cardiac I_{Ks} potassium channel. Nature 1996; 384:80–83.
6. Abbott GW, Sesti F, Splawski I, et al. MiRP1 forms I_{Kr} potassium channels with HERG and is associated with cardiac arrhythmia. Cell 1999;97:175–187.
7. Sesti F, Abbott GW, Wei J, et al. A common polymorphism associated with antibiotic-induced cardiac arrhythmia. Proc Natl Acad Sci U S A 2000;97: 10613–10618.
8. Tinel N, Diochot S, Borsotto M, Lazdunski M, Barhanin J. *KCNE2* confers background current characteristics to the cardiac KCNQ1 potassium channel. EMBO J 2000;19:6326–6330.
9. Wu DM, Jiang M, Zhang M, Liu XS, Korolkova YV, Tseng GN. *KCNE2* is colocalized with KCNQ1 and *KCNE1* in cardiac myocytes and may function as a negative modulator of $I_{(Ks)}$ current amplitude in the heart. Heart Rhythm 2006;3:1469–1480.
10. Toyoda F, Ueyama H, Ding WG, Matsuura H. Modulation of functional properties of KCNQ1 channel by association of KCNE1 and KCNE2. Biochem Biophys Res Commun 2006;344:814–820.
11. Yu H, Wu J, Potapova I, et al. MinK-related peptide 1: a beta subunit for the HCN ion channel subunit family enhances expression and speeds activation. Circ Res 2001;88:E84–E87.
12. McCrossan ZA, Roepke TK, Lewis A, Panaghie G, Abbott GW. Regulation of the Kv2.1 potassium channel by MinK and MiRP1. J Membr Biol 2009;228:1–14.
13. Zhang M, Jiang M, Tseng GN. MinK-related peptide 1 associates with Kv4.2 and modulates its gating function: potential role as beta subunit of cardiac transient outward channel? Circ Res 2001;88:1012–1019.
14. Delpon E, Cordeiro JM, Nunez L, et al. Functional effects of KCNE3 mutation and its role in the development of Brugada syndrome. Circ Arrhythm Electrophysiol 2008;1:209–218.
15. Roepke TK, Kontogeorgis A, Ovanez C, et al. Targeted deletion of *KCNE2* impairs ventricular repolarization via disruption of $I_{K,slow1}$ and $I_{to,f}$. FASEB J 2008;22:3648–3660.
16. Calloe K, Cordeiro JM, Di Diego JM, et al. A transient outward potassium current activator recapitulates the electrocardiographic manifestations of Brugada syndrome. Cardiovasc Res 2009;81:686–694.
17. Dixon JE, Shi W, Wang HS, et al. Role of the Kv4.3 K^+ channel in ventricular muscle. A molecular correlate for the transient outward current. Circ Res 1996;79:659–668.
18. Kääb S, Dixon J, Duc J, et al. Molecular basis of transient outward potassium current downregulation in human heart failure: a decrease in Kv4.3 mRNA correlates with a reduction in current density. Circulation 1998;98:1383–1393.
19. Benitah JP, Gomez AM, Bailly P, et al. Heterogeneity of the early outward current in ventricular cells isolated from normal and hypertrophied rat hearts. J Physiol 1993;469:111–138.
20. Singleton CB, Valenzuela SM, Walker BD, et al. Blockade by N-3 polyunsaturated fatty acid of the Kv4.3 current stably expressed in Chinese hamster ovary cells. Br J Pharmacol 1999;127:941–948.
21. Deschênes I, Tomaselli GF. Modulation of Kv4.3 current by accessory subunits. FEBS Lett 2002;528:183–188.
22. Wang S, Bondarenko VE, Qu Y, Morales MJ, Rasmusson RL, Strauss HC. Activation properties of Kv4.3 channels: time, voltage and $[K^+]_o$ dependence. J Physiol 2004;557:705–717.
23. An WF, Bowlby MR, Betty M, et al. Modulation of A-type potassium channels by a family of calcium sensors. Nature 2000;403:553–556.
24. Decher N, Uyguner O, Scherer CR, et al. hKChIP2b is a functional modifier of hKv4.3 potassium channels: cloning and expression of a short hKChIP2b splice variant. Cardiovasc Res 2001;52:255–264.
25. Radicke S, Cotella D, Graf EM, et al. Functional modulation of the transient outward current I_{to} by *KCNE* beta-subunits and regional distribution in human non-failing and failing hearts. Cardiovasc Res 2006;1:695–703.
26. Deschênes I, DiSilvestre D, Juang GJ, Wu RC, An WF, Tomaselli GF. Regulation of Kv4.3 current by KChIP2b splice variants: a component of native cardiac I_{to}? Circulation 2002;106:423–429.
27. Radicke R, Vaquero M, Caballero R, et al. Effects of MiRP1 and DPP6 β-subunits on the blockade induced by flecainide of Kv4.3/KChIP2 channels. Br J Pharmacol 2008;154:774–786.
28. Wettwer E, Amos GJ, Posival H, Ravens U. Transient outward current in human ventricular myocytes of subepicardial and subendocardial origin. Circ Res 1994; 75:473–482.
29. Patel SP, Campbell DL. Transient outward potassium current, "I_{to}," phenotypes in the mammalian left ventricle: underlying molecular, cellular and biophysical mechanisms. J Physiol 2005;569:7–39.
30. Antzelevitch C. Brugada syndrome. Pacing Clin Electrophysiol 2006;29:1130–1159.
31. Bezzina C, Veldkamp MW, van den Berg MP, et al. A single Na^+ channel mutation causing both long-QT and Brugada syndromes. Circ Res 1999;85: 1206–1213.
32. Van den Berg MP, Wilde AA, Viersma TJW, et al. Possible bradycardic mode of death and successful pacemaker treatment in a large family with features of long QT syndrome type 3 and Brugada syndrome. J Cardiovasc Electrophysiol 2001;12:630–636.

Long QT syndrome with compound mutations is associated with a more severe phenotype: A Japanese multicenter study

Hideki Itoh, MD, PhD,* Wataru Shimizu, MD, PhD,† Kenshi Hayashi, MD, PhD,‡ Kenichiro Yamagata, MD,† Tomoko Sakaguchi, MD, PhD,* Seiko Ohno, MD, PhD,§ Takeru Makiyama, MD, PhD,§ Masaharu Akao, MD, PhD,§ Tomohiko Ai, MD, PhD,¶ Takashi Noda, MD, PhD,† Aya Miyazaki, MD,‖ Yoshihiro Miyamoto, MD, PhD,** Masakazu Yamagishi, MD, PhD,‡ Shiro Kamakura, MD, PhD,† Minoru Horie, MD, PhD*

*From the *Department of Cardiovascular and Respiratory Medicine, Shiga University of Medical Science, Otsu, Japan, †Division of Arrhythmia and Electrophysiology, Department of Cardiovascular Medicine, National Cerebral and Cardiovascular Center, Suita, Japan, ‡Division of Cardiovascular Medicine, Kanazawa University Graduate School of Medical Science, Kanazawa, Japan, §Department of Cardiovascular Medicine, Kyoto University Graduate School of Medicine, Kyoto, Japan, ¶Texas Heart Institute/St. Luke's Episcopal Hospital, Houston, Texas, ‖Department of Pediatric Cardiology, National Cerebral and Cardiovascular Center, Suita, Japan, and **Laboratory of Molecular Genetics, National Cerebral and Cardiovascular Center, Suita, Japan.*

BACKGROUND: Long QT syndrome (LQTS) can be caused by mutations in the cardiac ion channels. Compound mutations occur at a frequency of 4% to 11% among genotyped LQTS cases.

OBJECTIVE: The purpose of this study was to determine the clinical characteristics and manner of onset of cardiac events in Japanese patients with LQTS and compound mutations.

METHODS: Six hundred three genotyped LQTS patients (310 probands and 293 family members) were divided into two groups: those with a single mutation (n = 568) and those with two mutations (n = 35). Clinical phenotypes were compared between the two groups.

RESULTS: Of 310 genotyped probands, 26 (8.4%) had two mutations in the same or different LQTS-related genes (compound mutations). Among the 603 LQTS patients, compound mutation carriers had significantly longer QTc interval (510 ± 56 ms vs 478 ± 53 ms, $P = .001$) and younger age at onset of cardiac events (10 ± 8 years vs 18 ± 16 years, $P = .043$) than did single mutation carriers. The incidence rate of cardiac events before age 40 years and use of beta-blocker therapy among compound mutation carriers also were different than in single mutation carriers. Subgroup analysis showed more cardiac events in LQTS type 1 (LQT1) and type 2 (LQT2) compound mutations compared to single LQT1 and LQT2 mutations.

CONCLUSION: Compound mutation carriers are associated with a more severe phenotype than single mutation carriers.

KEYWORDS Compound; Gene; Long QT syndrome; Mutation

ABBREVIATION QTS = long QT syndrome

(Heart Rhythm 2010;7:1411–1418)

Introduction

Congenital long QT syndrome (LQTS) is a heterogeneous disease characterized by prolonged ventricular repolarization and episodes of syncope and/or life-threatening cardiac arrhythmias, particularly polymorphic ventricular tachycardia.[1] Several disease-causing genes have been identified, including genes encoding cardiac ion channel-composing proteins, namely, *KCNQ1* (LQT1), *KCNH2* (LQT2), *SCN5A* (LQT3), *KCNE1* (LQT5), *KCNE2* (LQT6), *KCNJ2* (LQT7), and *CACNA1C* (LQT8), and genes encoding a family of versatile membrane adapters, namely, *ANK2* (LQT4), *CAV3* (LQT9), *SCN4B* (LQT10), *AKAPs* (LQT11), and *SNTA1* (LQT12).[2–5] Two modes of inheritance are involved in this syndrome, which exhibits both an autosomal dominant and an autosomal recessive pattern. The majority of LQTS cases are inherited in an autosomal dominant fashion. This pattern, which has been named as Romano-Ward syndrome,[6,7] can result from a single mutation in one

Drs. Shimizu, Makiyama, Akao, Miyazaki, Miyamoto, Yamagishi, and Horie were supported in part by a Health Sciences Research Grant (H18-Research on Human Genome-002) and a Research Grant for the Cardiovascular Diseases (21C-8) from the Ministry of Health, Labour and Welfare, Japan. Dr. Itoh was supported in part by a Grant-in-Aid for Young Scientists from the Ministry of Education, Culture and Technology. Dr. Horie was supported by the Uehara Memorial Foundation. Drs. Itoh and Shimizu contributed equally to this study. **Address reprint requests and correspondence:** Dr. Wataru Shimizu, Division of Arrhythmia and Electrophysiology, Department of Cardiovascular Medicine, National Cerebral and Cardiovascular Center, 5-7-1 Fujishiro-dai, Suita, Osaka 565-8565, Japan. E-mail address: wshimizu@hsp.ncvc.go.jp. (Received 7 February 2010; accepted June 3, 2010.)

1547-5271/$ -see front matter doi:10.1016/j.hrthm.2010.06.013

of the LQTS candidate genes. On the other hand, Jervell and Lange-Nielsen syndrome, which is inherited in an autosomal recessive fashion, is very rare,[8] affecting less than 1% of LQTS cases. It is caused by homozygous or compound heterozygous mutations of *KCNQ1* or *KCNE1*.[9,10]

Genetic analysis sometimes reveals two or more mutations in LQTS patients with clinical phenotypes of Romano-Ward syndrome. These compound mutations were shown to be associated with an increased arrhythmic risk.[11,12] However, most previous studies were conducted in Caucasian patients, and few systematic studies have involved Asian cohorts. In the present study, we analyzed the clinical characteristics of LQTS patients who were registered in a Japanese multicenter study. Analysis of the more 600 genotyped patients revealed that LQTS patients with compound mutations not only were common in Japan (8.4% among probands) but were associated with longer QTc and earlier onset of cardiac events. In patients who initially are diagnosed as LQT1 or LQT2, additional mutations may be present if patients have a more severe phenotype than expected; therefore, conducting a survey for major LQTS-related genes is critically important.

Methods

Patients and data collection

Major candidate genes were analyzed in 612 consecutive and unrelated probands with a suspected clinical diagnosis of congenital LQTS, who were referred to four centers in Japan (Shiga University of Medical Science, Otsu; Kyoto University Graduate School of Medicine, Kyoto; Kanazawa University Graduate School of Medical Science, Kanazawa; and National Cardiovascular Center, Suita) between June 1996 and January 2009. If gene mutations in LQTS-related genes were identified, further genetic analysis was conducted among family members as extensively as possible. All patients in the cohort were Japanese.

Genetic analysis

Informed consent was obtained from all individuals or their guardians according to standards established by the local institutional review boards. Genotypic and DNA sequence analyses of *KCNQ1, KCNH2, SCN5A, KCNE1,* and *KCNE2* were performed as described previously.[13] In addition, *KCNJ2* (Andersen syndrome [LQT7][14,15]) was analyzed in patients who had not only QT prolongation but also the clinical phenotype of Andersen syndrome, for example, periodic paralysis or dysmorphic features. Other candidate genes (e.g., ankyrin-B [LQT4], *CACNA1C* [Timothy syndrome, LQT8]) were not analyzed because mutations in these genes are extremely rare. Denaturing high-performance liquid chromatography was performed as described previously.[16] Abnormal conformers were amplified by polymerase chain reaction and sequenced using an ABI PRISM310 DNA sequencer (Perkin-Elmer Applied Biosystems, Wellesley, MA, USA). "Splicing error" mutations were defined as those that occurred within three bases of the splicing sites. When mutations were detected, 200 Japanese control subjects were checked and single nucleotide polymorphisms were excluded from the study. If mutations of these genes were detected in the probands, their family members were also analyzed and genotype–phenotype correlations confirmed. Mutation-negative controls were defined as family members without mutations detected in each proband. Nonsynonymous as well as synonymous single nucleotide polymorphisms were excluded with the assistance of data from previous reports[17–19] and from the National Center for Biotechnology Information database.

Clinical characterization

Baseline clinical data were recorded for each patient and included the following: age at diagnosis, age at first cardiac event, sex, cardiac events, family history of sudden cardiac death or LQTS members, ECG measurements, and therapeutic regimens administered. Schwartz scores also were calculated.[20,21] In the analysis of triggers of arrhythmic events, triggers were divided into four categories: exercise/swimming, emotional stress/arousal stress, sleep/rest, and other conditions.

ECG parameters measured at baseline included RR, QT_{end}, QT_{peak}, and $T_{peak\text{-}end}$ ($QT_{end\text{-}peak}$) intervals. The latter is thought to reflect transmural dispersion of ventricular repolarization.[22] Measurements were the mean of at least three beats measured in lead V_5 from the 12-lead ECG during stable sinus rhythm and corrected by the Bazett formula.[23] QT_{end} was manually measured as the time interval between QRS onset (Q) and the point at which the isoelectric line intersected a tangential line drawn at the maximal downslope of the positive T wave or the maximal

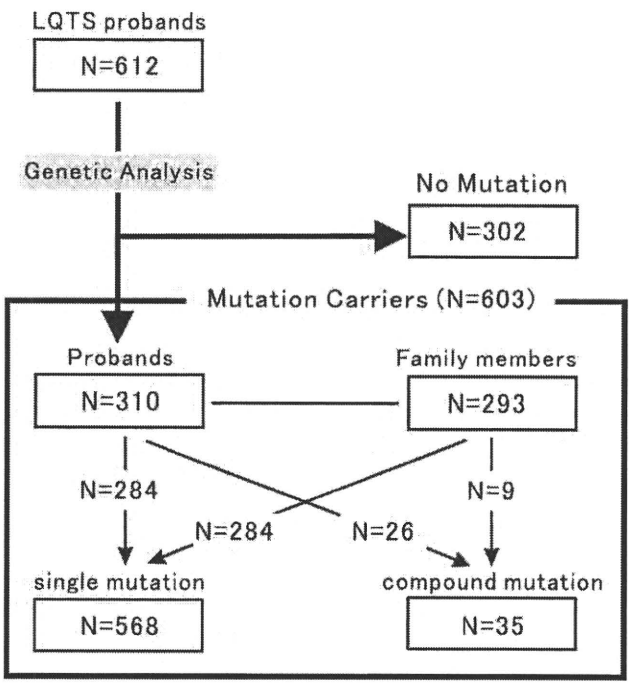

Figure 1 Schematic representation of the positive-mutation carriers in this study. LQTS = long QT syndrome.

Table 1 Overall data of patients with compound mutations

Research groups	Schwartz et al.	Westenkow et al.	Tester et al.	This study
Reported years	2003	2004	2005	2010
The corresponding number in the reference list	25	11	12	
Percentage of probands with compound mutations (probands with compound mutations/total probands) subtypes	4.6% (6/130)	5.2% (9/172*)	10.8% (29/269)	8.4% (26/310)
LQT1	7 (58%)	14 (35%)	30 (52%)	18 (35%)
LQT2	2 (17%)	10 (25%)	15 (26%)	17 (33%)
LQT3	3 (25%)	2 (5%)	13 (22%)	14 (27%)
LQT5-D85N	0 (0%)	10 (25%)	0 (0%)	0 (0%)
vs. single mutation carriers				
QTc interval	NA	prolonged	not significant	prolonged
Cardiac events	NA	frequent	not significant	not significant
Age of onset	NA	NA	younger onset	younger onset

*This table excluded probands with single nucleotide polymorphisms (SNP), NA = not available.

upslope of the negative T wave (QT_{end}). $QT_{end\text{-}peak}$ then was obtained by calculating as QT_{end} minus QT_{peak}.

Statistical analysis

All analyses were performed using the SPSS 16.0 statistical package (SPSS, Inc., Chicago, IL. USA). Data are expressed as mean ± SD. $P < 0.05$ was considered significant. Univariate comparison of parameters between groups was performed by an unpaired t-test. Differences in incidence between groups were analyzed by Chi-square test or Fisher exact probability test. The cumulative probability of a first cardiac event (syncope, torsades de pointes, ventricular fibrillation, cardiac arrest, or sudden death) occurring before age 40 years and before beta-blocker therapy or after beta-blocker therapy was determined by means of the life-table method of Kaplan-Meier, and results were compared using log rank test.[24]

Results

Genetic characteristics of mutations associated with single and compound mutations

Genetic analysis revealed gene mutations in 310 (51%) of 612 probands. The study enrolled 603 genotyped LQTS patients consisting of 310 genotyped probands and their 293 genotyped family members. A flowchart of the genetic diagnosis of the study population is shown in Figure 1.

Of the 310 genotyped probands, 26 (8.4%) had compound mutations. This rate is comparable to the rates in previous reports of Caucasian patients (Table 1). The 26 probands all had two mutations in the LQTS-related genes we examined. These 52 mutations in 26 probands consisted of 45 missense mutations, 4 frameshift mutations, 2 splice-site mutations, and 1 nonsense mutation (see Online Supplemental Data 1). The mutation types of the 284 single mutation carriers were 210 missense mutations, 34 frameshift mutations, 18 splicesite mutations, 12 deletions, 9 nonsense mutations, and 1 insertion mutation (see Online Supplemental Data 2). Therefore, the mutation types were similar between the two groups (Figure 2).

Among the 293 genotyped family members, there were 284 single mutation carriers and 9 compound mutation carriers. In total, 568 patients with a single mutation (284 probands and 284 family members) consisted of 256 with LQT1, 248 with LQT2, 62 with LQT3, and 2 with LQT5. Thirty-five compound mutation carriers (26 probands and 9 family members) consisted of 9 with LQT2 and LQT3, 7 with LQT1 and LQT2, 6 with LQT1 and LQT3, 4 with double LQT1, 3 with double LQT2 mutations, 2 with LQT1 and LQT7, 2 with LQT2 and LQT7, 1 with double LQT3, and 1 with LQT1 and LQT6.

Families associated with compound mutations

In the analysis of family members associated with compound mutations, 28 single heterozygous mutation carriers and 4 obligate single mutation carriers were identified from 9 families, and single mutation carriers had milder clinical phenotypes than compound mutation carriers (Figure 3). Only 2 (6%) of the 32 single mutation carriers had syncope but no torsades de pointes, an incidence lower than that in compound mutation carriers (54% [19/35] patients, $P < .001$). For single heterozygous mutation carriers in compound mutation families, average QTc interval was 442 ± 30 ms, which was longer than that of the 15 mutation-negative controls (408 ± 28 ms, $P = .001$) but significantly shorter than that of compound mutation carriers (510 ± 56 ms, $P < .001$).

Early onset of cardiac events and more severe QT prolongation was observed in patients with compound mutations

Table 2 compares the clinical characteristics of 35 LQTS patients with compound mutation and 568 LQTS patients with a single mutation. The female-to-male ratio was similar between the two groups. However, the incidence of family members associated with double-hit patients was significantly smaller than that with a single mutation (26% vs 50%, $P = .005$). In the ECG analysis of 496 patients with available information, corrected QT interval was significantly longer in compound mutation carriers than in single mutation carriers (510 ± 56 ms vs 478 ± 53 ms, respectively, $P = .001$), whereas other ECG findings, R-R interval, corrected QT_{peak}, corrected $QT_{peak\text{-}end}$, and rates of

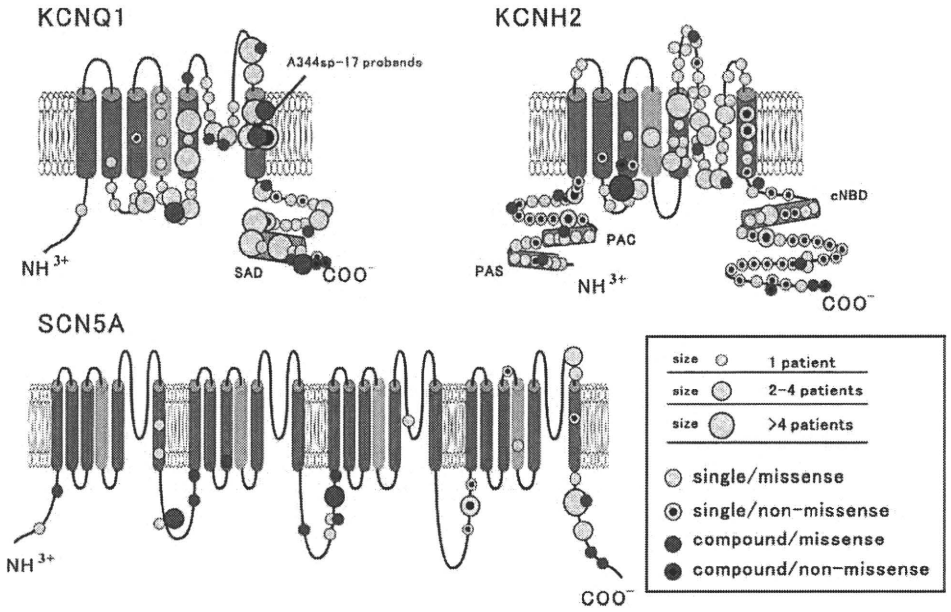

Figure 2 Conventional transmembrane topology of all mutations in the probands.

notched T wave and T-wave alternans were not different between the two groups. The frequency of patients with a normal QTc interval <440 ms was similar between the two groups, whereas the frequency of double-hit patients with QTc intervals >500 ms was significantly higher than in those with a single mutation (66% vs 26%, P <.001). Schwartz scores in the compound mutation group and the rate of patients with a score ≥4 were higher than those in the single mutation group (Schwartz score: 4.3 ± 2.1 vs 3.4 ± 1.9 points, P = .017; rates of Schwartz score ≥4 points: 70% vs 47%, P = .026). A significantly higher number of patients with compound mutations received beta-blocker therapy than did those with a single mutation (56% vs 33%, P = .006).

In the analysis of "all age groups," the frequency of cardiac events was similar between compound and single mutation groups, whereas age at first cardiac event was significantly lower in the compound mutation group (10 ± 8 years vs 18 ± 16 years, P = .043). For the occurrence of syncope or torsades de pointes before age 40 years, compound mutation carriers had significantly more events than did single mutation carriers (54% vs 37%, P = .043). The occurrence of cardiac arrest or ventricular fibrillation was similar between the two groups for patients before age 40 years. In 561 patients with available information on age at first cardiac events, Kaplan-Meier analysis showed that the cumulative rate of survival without a cardiac event before age 40 years and use of beta-blocker therapy differed significantly between compound and single mutation carriers (P = .004 by log rank test; Figure 4A) and between compound mutation carriers and each subgroup of single mutation carriers (P = .004 vs LQT1, P = .018 vs LQT2, P = .001 vs LQT3, by log rank test; Figure 4B). In the analysis of matched subtypes between single and compound mutation carriers, patients with additional mutations in an LQTS subtype had a significantly poorer prognosis than LQT1 alone (P = .001; Figure 5) and LQT2 alone (P = .035) but not LQT3 alone (P = .06).

Discussion

In this multicenter study, the major findings were as follows. (1) LQTS-associated compound mutations in the Japanese population were as common as previously reported in studies of Caucasian patient cohorts. (2) Patients with compound mutations displayed longer QTc and earlier onset of cardiac events. (3) Patients with compound mutations had more cardiac events before age 40 years and more beta-blocker therapy. (4) Subgroup analysis showed more cardiac events in LQT1 and LQT2 compound mutations compared to single LQT1 and LQT2 mutations.

Twenty-six probands (8.4% of genotyped LQTS) were found to have two variants in genes encoding ion channels *(KCNQ1, KCNH2, SCN5A, KCNE1, KCNE2,* or *KCNJ2).* This incidence rate is in general agreement with other studies that reported a prevalence of compound or multiple mutations of 5% to 11% of genotyped LQTS (Table 1).[11,18,25]

Table 1 summarizes the genetic and clinical characteristics of patients enrolled in previous studies and compares them with the characteristics of patients enrolled in the present study. Sanguinetti and colleagues reported that patients with compound mutations not only had longer QT intervals than single mutation carriers but also had more frequent cardiac events.[11] However, Ackerman and colleagues demonstrated that, although compound mutation carriers were diagnosed at a younger age than single mutation carriers, they did not have significantly longer QT intervals.[12] The difference between these results might be explained by half of the 20 compound probands in the cohort of Sanguinetti et al possessing the common *KCNE1-*

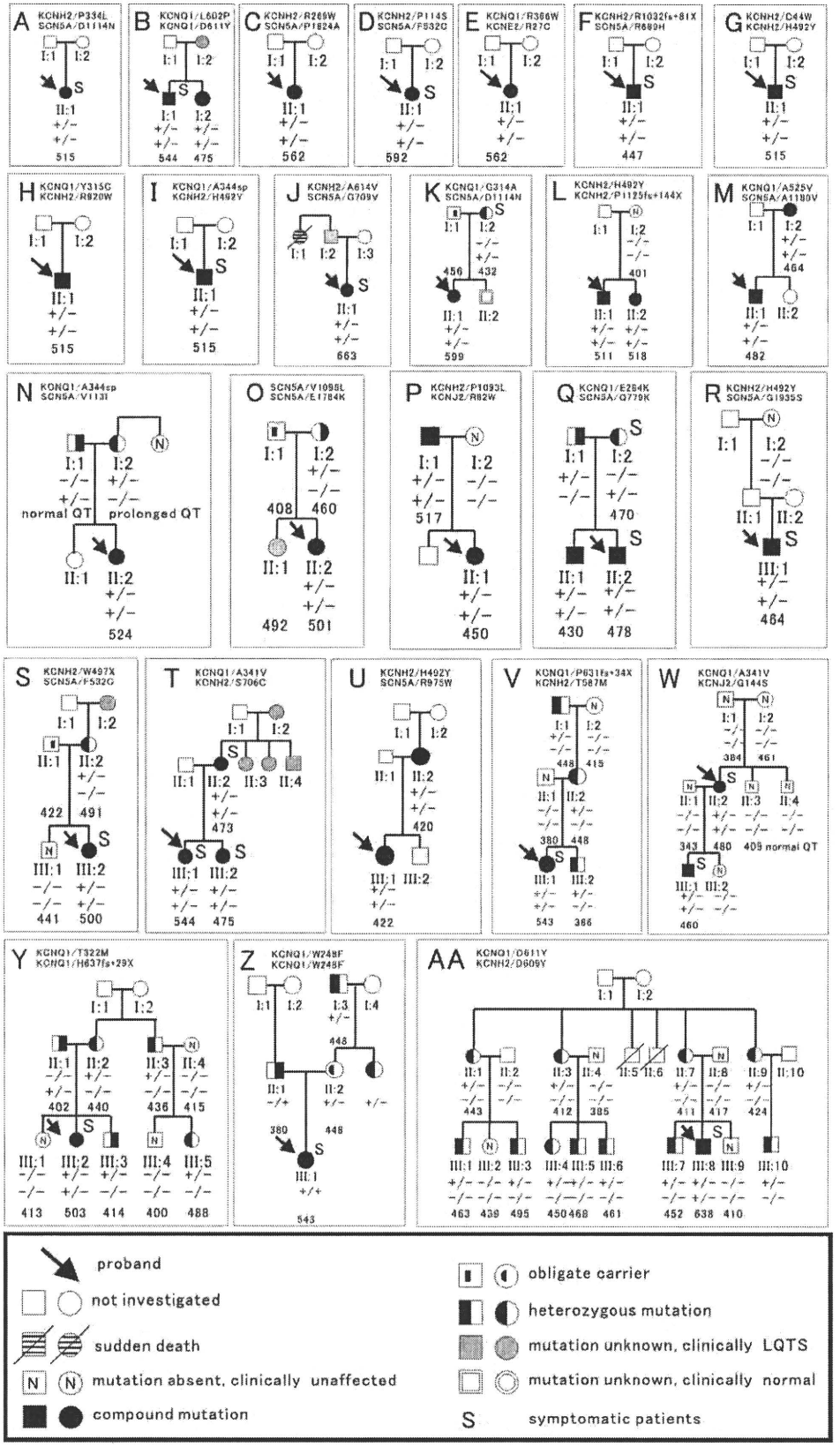

Figure 3 Pedigrees of the families associated with compound mutation probands.

Table 2 Clinical characteristics of LQTS patients with gene mutations

	Compound mutations (N=35)	Single mutations (N=568)	p value
Demographic			
Age at diagnosis (yrs)	19 ± 14 [15, 9-27]	28 ± 19 [22, 12-42]	0.001
Female gender	23 (66%)	330 (58%)	0.394
Proband	26 (74%)	284 (50%)	0.005
Family members	9 (26%)	284 (50%)	0.005
Cardiac events			
cardiac events in all age groups			
Age at first cardiac event (yrs)	10 ± 8 [11, 3.5-13.5]	18 ± 16 [12, 7-19]	0.043
syncope	19 (54%)	235 (41%)	0.161
TdP	10 (29%)	102 (18%)	0.136
cardiac arrest or VF	3 (9%)	44 (8%)	0.748
sudden death	0 (0%)	4 (1%)	1.000
cardiac events before 40 yrs			
syncope or TdP	19 (54%)	205 (37%)	0.043
cardiac arrest or VF	3 (9%)	37 (7%)	0.500
ECG measurements			
RR interval (ms)	866 ± 210	914 ± 174	0.252
corrected QT (ms)	510 ± 56	478 ± 53	0.001
corrected QT >500 ms (%)	23 (66%)	122 (26%)	<0.001
corrected QT <440 ms (%)	3 (9%)	91 (20%)	0.351
corrected QT peak (ms)	385 ± 70	384 ± 50	0.906
corrected QT peak-end (ms)	121 ± 73	95 ± 41	0.081
notched T wave	11 (31%)	200 (37%)	0.540
T-wave alternans	0 (0%)	30 (5%)	0.246
Diagnosis			
Schwartz score	4.2 ± 2.1	3.4 ± 1.9	0.017
Schwartz score ≧4	21 (70%)	219 (47%)	0.026
Therapy			
β-blocker	10 (56%)	175 (33%)	0.006
class Ib antiarrhythmic drugs	3 (9%)	53 (10%)	1.000
pacemaker	1 (3%)	15 (3%)	1.000
sympathectomy	1 (3%)	3 (1%)	0.218
defibrillator	1 (3%)	32 (6%)	0.712

TdP = torsades de pointes, VF = ventricular fibrillation, NS = not significant, corrected QT = QT interval corrected for heart rate with Bazett formula [A, B], A = median, B-C = first interquartile range-third interquartile range.

D85N polymorphism as the "second hit" (Table 1).[11,26] In all age groups of this study, the incidence of cardiac events, such as torsades de pointes or syncope, was similar between single and compound mutation carriers; however, the clinical phenotypes of those with compound mutations before 40 years of age were more serious than in those with a single mutation (Table 2). Thus, phenotypes with compound mutations appear to be more serious than single mutation carriers, regardless of race.

Beta-blocker therapy is first-line treatment for the prevention of cardiac events in LQTS. Beta-blockers have been shown to significantly reduce cardiac events in LQTS patients, especially LQT1 type.[27–29] However, patients with LQT2 or LQT3 have been reported to be less responsive to beta-blocker therapy[27,30] and may require additional therapy, such as pacemaker implantation for LQT2 or a Class Ib antiarrhythmic drug for LQT3. It may be recommended that patients with compound mutations receive additional individual therapy based on their LQTS subtype, for example, the combination of beta-blocker and Class Ib antiarrhythmic drugs for patients with LQT1 and LQT3. In patients who were first diagnosed as LQT1, Kobori et al[31] reported that additional mutations in different LQTS-related genes influenced phenotype severity and reduced beta-blocker effectiveness. Previous reports showed that approximately 20% of LQT1 patients were resistant to beta-blocker therapy. Additional or "latent" mutations may be present in these patients, and conducting a survey for major all LQTS-related genes, even after a possible mutation is identified, is critically important.

Family study analyses are of enormous importance because single mutation carriers in this study tended to have mild phenotypes. Most of the single mutation carriers in families of compound probands remained asymptomatic. However, double hits of these "latent" gene carriers could cause more serious phenotypes.[32,33] Jervell and Lange-Nielsen syndrome is a well-documented LQTS phenotype with an autosomal recessive pattern. The loss of function of I_{Ks} on both alleles generally causes not only more severe clinical phenotypes but also deafness.[9,10] In our study, two of three probands with double *KCNQ1* mutations had no deafness. We speculate that these mutations would functionally cause mild changes without complete loss of I_{Ks}. Westenskow et al[11] reported the molecular mechanism of

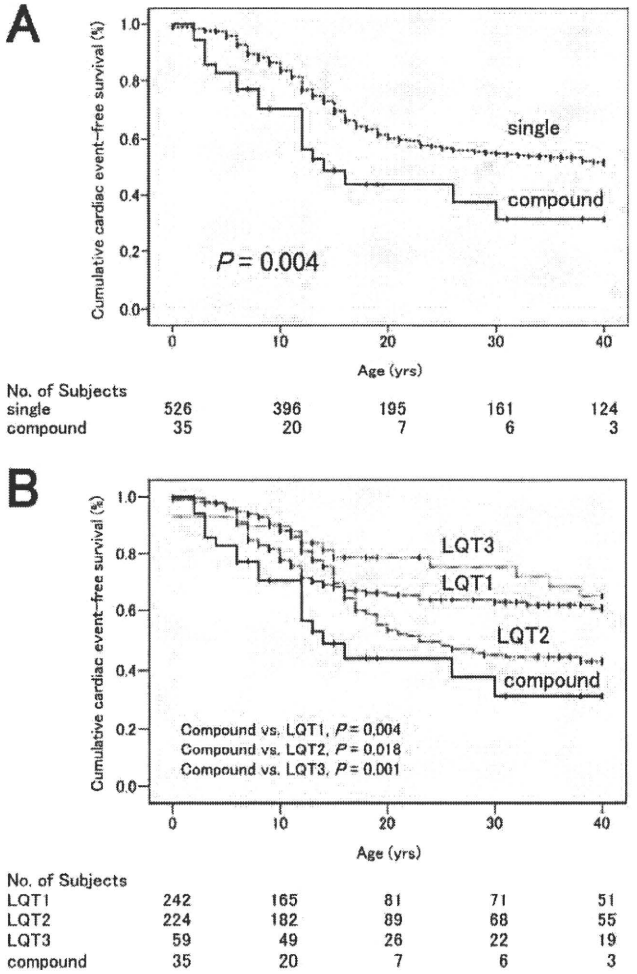

Figure 4 Kaplan-Meier cumulative probability of cardiac event-free survival from birth to age 40 years and before therapy. **A:** Comparison between patients with a single mutation and compound mutations. **B:** Comparison among patients with long QT syndrome type 1 (LQT1), type 2 (LQT2), type 3 (LQT3), and compound mutations.

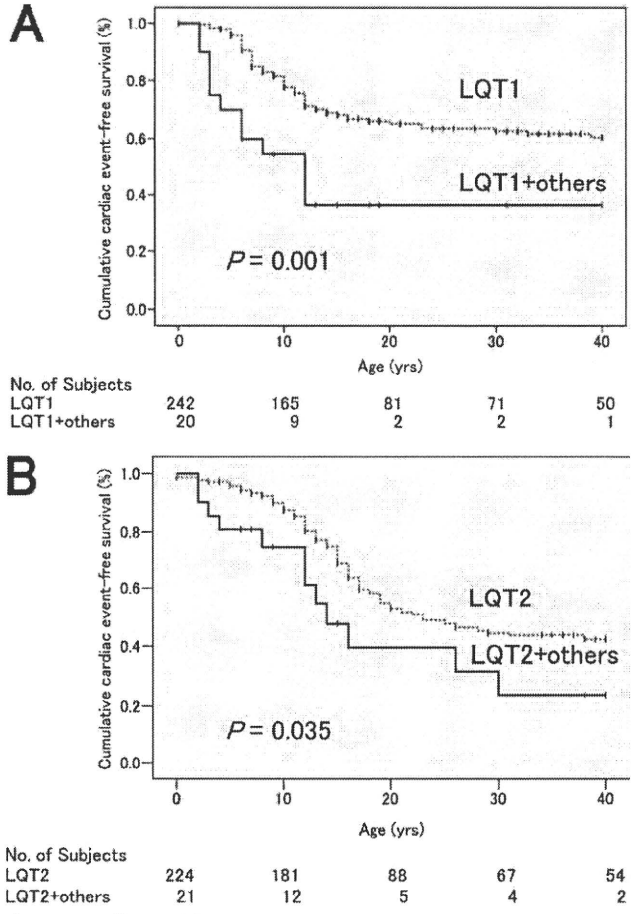

Figure 5 Kaplan-Meier cumulative probability of cardiac event-free survival from birth to 40 years of age and before therapy. **A:** Comparison between patients with long QT type 1 (LQT1_ subtype and compound mutation carriers with LQT1 plus other mutations. **B:** Comparison between patients with long QT syndrome type 2 (LQT2) and those with LQT2 plus other mutations.

increased risk through compound mutations using heterologous expressions in *Xenopus* oocytes. When wild-type and variant subunits were coexpressed in appropriate ratios to mimic the genotype of the probands with mutations, the reduction in current density was equivalent to the additive effects of the single mutations. Coexpression of two mutant subunits caused a significant but incomplete reduction. Thus, either compound mutation seems to be associated with mild functional damage. It is necessary to have "double hits" of these mild mutations in order to produce symptoms.

Study limitations

This study has several limitations. First, six major LQTS candidate genes were examined, but not for minor genes encoding a family of versatile membrane adapters. However, excluding these minor genes from our investigations would not have affected the overall study results, largely because the incidence of these minor gene mutations reportedly is ≤1%. Second, analysis of single mutation carriers in compound mutation families is dominated by their presence in only 35% (9/26) of families. Therefore, there might be a statistical bias due to a mutation-specific effect. Third, Kapa et al[19] reported the need for further studies on whether regions such as the interdomain linker of *SCN5A* could affect the clinical phenotypes of LQTS. In this study, we were able to distinguish mutations from these "genetic noises," especially in the *SCN5A* gene.

Acknowledgment

We thank Professor Pascale Guicheney (INSERM, U956, Group Hospitalier Pitié-Salpêtrière, Paris) for advice and review of the manuscript.

Appendix

Supplementary data

Supplementary data associated with this article can be found, in the online version, at doi:10.1016/j.hrthm.2010.06.013.

References

1. Moss AJ, Zareba W. Long QT syndrome: therapeutic considerations. In: Zipes DP, Jalife J, editors. Cardiac Electrophysiology: From Cell to Bedside. Philadelphia: WB Saunders, 2004:660–667.

2. Shimizu W. Clinical impact of genetic studies in lethal inherited cardiac arrhythmia. Circ J 2008;72:1926–1936.
3. Goldenberg I, Moss AJ. Long QT syndrome. J Am Coll Cardiol 2008;51:2291–2300.
4. Chen L, Marquardt ML, Tester DJ, Sampson KJ, Ackerman MJ, Kass RS. Mutation of an A-kinase-anchoring protein causes long-QT syndrome. Proc Natl Acad Sci U S A 2007;104:20990–20995.
5. Ueda K, Valdivia C, Medeiros-Domingo A, et al. Syntrophin mutation associated with long QT syndrome through activation of the nNOS-SCN5A macromolecular complex. Proc Natl Acad Sci U S A 2008;105:9355–9360.
6. Romano C, Gemme G, Pongigione R. Aritmie cardiache rare in'eta pediatrica. Clin Pediatr 1963;45:658.
7. Ward OC. A new familial cardiac syndrome in children. J Irish Med Assoc 1964;54:103.
8. Jervell A, Lange-Nielsen F. Congenital deaf-mutism, functional heart disease with prolongation of the Q-T interval and sudden death. Am Heart J 1957;54:59–68.
9. Neyroud N, Tesson F, Denjoy I, et al. A novel mutation in the potassium channel gene KVLQT1 causes the Jervell and Lange-Nielsen cardioauditory syndrome. Nat Genet 1997;15:186–189.
10. Schulze-Bahr E, Wang Q, Wedekind H, et al. KCNE1 mutations cause Jervell and Lange-Nielsen syndrome. Nat Genet 1997;17:267–268.
11. Westenskow P, Splawski I, Timothy KW, Keating MT, Sanguinetti MC. Compound mutations: a common cause of severe long-QT syndrome. Circulation 2004;109:1834–1841.
12. Tester DJ, Will ML, Haglund CM, Ackerman MJ. Compendium of cardiac channel mutations in 541 consecutive unrelated patients referred for long QT syndrome genetic testing. Heart Rhythm 2005;2:507–517.
13. Ohno S, Zankov DP, Yoshida H, et al. N- and C-terminal KCNE1 mutations cause distinct phenotypes of long QT syndrome. Heart Rhythm 2007;4:332–340.
14. Ai T, Fujiwara Y, Tsuji K, et al. Novel KCNJ2 mutation in familial periodic paralysis with ventricular dysrhythmia. Circulation 2002;105:2592–2594.
15. Andelfinger G, Tapper AR, Welch RC, Vanoye CG, George AL Jr, Benson DW. KCNJ2 mutation results in Andersen syndrome with sex-specific cardiac and skeletal muscle phenotypes. Am J Hum Genet 2002;71:663–668.
16. Jongbloed R, Marcelis C, Velter C, Doevendans P, Geraedts J, Smeets H. DHPLC analysis of potassium ion channel genes in congenital long QT syndrome. Hum Mutat 2002;20:382–391.
17. Ackerman MJ, Tester DJ, Jones GS, Will ML, Burrow CR, Curran ME. Ethnic differences in cardiac potassium channel variants: implications for genetic susceptibility to sudden cardiac death and genetic testing for congenital long QT syndrome. Mayo Clin Proc 2003;78:1479–1487.
18. Kapplinger JD, Tester DJ, Salisbury BA, et al. Spectrum and prevalence of mutations from the first 2500 consecutive unrelated patients referred for the FAMILION long QT syndrome genetic test. Heart Rhythm 2009;6:1297–1303.
19. Kapa S, Tester DJ, Salisbury BA, et al. Genetic testing for long-QT syndrome: distinguished pathogenic mutations from benign variants. Circulation 2009;120:1752–1760.
20. Schwartz PJ, Moss AJ, Vincent GM, Crampton RS. Diagnostic criteria for the long QT syndrome. Circulation 1993;88:782–784.
21. Moss AJ, Robinson J. Clinical features of the idiopathic Long-QT syndrome. Circulation 1992;85:I140–I144.
22. Shimzu W, Antzelevitch C. Sodium channel block with mexiletine is effective in reducing dispersion of repolarization and preventing torsade des pointes in LQT2 and LQT3 models of the long-QT syndrome. Circulation 1997;96:2038–2047.
23. Bazett H. An analysis of the time relations of electrocardiograms. Heart 1920;7:353–367.
24. Zareba W, Moss AJ, Locati EH, et al; International Long QT Syndrome Registry. Modulating effects of age and gender on the clinical course of long QT syndrome by genotype. J Am Coll Cardiol 2003;42:103–109.
25. Schwartz PJ, Priori SG, Napolitano C. How really rare are rare disease?: the intriguing case of independent compound mutations in the long QT syndrome. J Cardiovasc Electrophysiol 2003;14:1120–1121.
26. Nishio Y, Makiyama T, Itoh H, et al. D85N, a KCNE1 polymorphism, is a disease-causing gene variant in long QT syndrome. J Am Coll Cardiol 2009;54:812–819.
27. Priori SG, Napolitano C, Schwartz PJ, et al. Association of long QT syndrome loci and cardiac events among patients treated with beta-blockers. JAMA 2004;292:1341–1344.
28. Vincent GM, Schwartz PJ, Denjoy I, et al. High efficacy of beta-blockers in long-QT syndrome type 1: contribution of noncompliance and QT-prolonging drugs to the occurrence of beta-blocker treatment "failures." Circulation 2009;119:215–221.
29. Moss AJ, Shimizu W, Wilde AA, et al. Clinical aspects of type-1 long-QT syndrome by location, coding type, and biophysical function of mutations involving the KCNQ1 gene. Circulation 2007;115:2481–2489.
30. Shimizu W, Moss AJ, Wilde AA, et al. Genotype-phenotype aspects of type 2 long-QT syndrome. J Am Coll Cardiol 2009;54:2052–2062.
31. Kobori A, Sarai N, Shimizu W, et al. Additional gene variants reduce effectiveness of beta-blockers in the LQT1 form of long QT syndrome. J Cardiovasc Electrophysiol 2004;15:190–199.
32. Priori SG, Schwartz PJ, Napolitano C, et al. A recessive variant of the Romano-Ward long-QT syndrome? Circulation 1999;97:2420–2425.
33. Berthet M, Denjoy I, Donger C, et al. C-terminal HERG mutations: the role of hypokalemia and a KCNQ1-associated mutation in cardiac event occurrence. Circulation 1999;99:1464–1470.

P wave and the development of atrial fibrillation

Katsuya Ishida, MD,* Hideki Hayashi, MD, PhD,* Akashi Miyamoto, MD,* Yoshihisa Sugimoto, MD, PhD,* Makoto Ito, MD, PhD,* Yoshitaka Murakami, PhD,† Minoru Horie, MD, PhD*

*From the *Department of Cardiovascular and Respiratory Medicine, Shiga University of Medical Science, Shiga, Japan, and †Department of Health Science, Shiga University of Medical Science, Shiga, Japan.*

BACKGROUND Terminal P-wave inversion in lead V_1 representing left atrial overload has been considered a precursor of atrial fibrillation (AF).

OBJECTIVE The purpose of this study was to determine whether this P-wave morphologic characteristic can predict the development of AF.

METHODS Digital analysis of 12-lead ECGs was performed to enroll patients with P terminal force ≥0.06 s × 2 mm in lead V_1 from among a database of 308,391 ECG recordings. The prognostic value of ECG characteristics for developing AF was determined.

RESULTS A total of 78 patients (mean age 52 ± 19 years) with left atrial overload were chosen from among 102,065 patients in the database. During mean follow-up of 43 months, 15 (19%) patients developed AF (AF group) versus 63 (81%) patients who did not (non-AF group). No significant difference was noted between the AF and non-AF groups with regard to the area, duration, and amplitude of the P-wave terminal portion in lead V_1. In contrast, the area, duration, and amplitude of the P-wave initial portion in the same lead were significantly greater in the AF group than in the non-AF group (114.6 ± 73.0 μV × ms vs 73.1 ± 59.3 μV × ms, 42.2 ± 12.4 ms vs 35.7 ± 10.1 ms, and 94.0 ± 39.9 μV vs 68.8 ± 49.4 μV, respectively; $P < .05$ for each). Multivariate analysis confirmed that the area of the P-wave initial portion was independently associated with the development of AF (hazard ratio 4.02, 95% confidence interval 1.25–17.8; $P = .018$).

CONCLUSION P-wave initial portion in lead V_1 was an independent risk stratifier of AF development in patients with marked left atrial overload.

KEYWORDS Atrium; Electrocardiography; Fibrillation; Prognosis

ABBREVIATIONS **AF** = atrial fibrillation; **CI** = confidence interval; **ECG** = electrocardiogram; **LA** = left atrium; **RA** = right atrium

(Heart Rhythm 2010;7:289–294)

Introduction

The P wave reflects electrical depolarization of both the right atrium (RA) and the left atrium (LA). When the P wave is biphasic in lead V_1, the positive initial portion and the negative terminal portion of the P wave represent depolarization of the RA and the LA, respectively.[1,2] Morris et al[3] reported that the magnitude of the negative terminal potion of the P wave, calculated as the algebraic product of the duration and amplitude (P terminal force) in precordial lead V_1, was significantly larger in patients with various valvular heart diseases than in normal subjects. In their study, the P terminal force was associated with mitral valve area and increased LA pressure. The magnitude of the P terminal force has been shown to be associated with LA enlargement as revealed by transthoracic echocardiography.[4,5] These findings suggest that the negative terminal potion of the P wave in lead V_1 is a sign of pressure and volume overload in the LA, which may lead to structural and functional remodeling in the LA. Because atrial fibrillation (AF) often occurs and/or recurs in the remodeled LA,[6] the increased P terminal force may underlie the generation of AF. The increased P terminal force is observed not only in valvular heart diseases but also in other heart diseases, including hypertension, myocardial infarction, and cardiomyopathy.[7,8] These disorders potentially underlie the generation of AF. However, little is known about whether P terminal force occurring in those disorders is associated with a prognostic risk for the development of AF. Prolonged P-wave duration is a useful predictor of AF development.[9,10] The signal-averaged P-wave electrocardiogram (ECG) has a significant role in identifying patients who are susceptible to paroxysmal AF and in predicting the progression from paroxysmal to permanent AF.[11] Measurement of signal-averaged P-wave duration requires a dedicated system, which is not widely available in general clinical practice. In contrast, standard 12-lead ECGs can be conveniently recorded, and automatic analysis of 12-lead ECG recordings yields information to clinicians. In our university hospital, more than 300,000 ECGs obtained from more than 100,000 patients are available for digital analysis. Using this large database, we performed a retrospective cohort study to investigate whether terminal P-wave inversion in lead V_1 predicts the development of AF.

Address reprint requests and correspondence: Dr. Hideki Hayashi, Department of Cardiovascular and Respiratory Medicine, Shiga University of Medical Science, Otsu, Shiga 520-2192, Japan. E-mail address: hayashih@belle.shiga-med.ac.jp. (Received October 11, 2009; accepted November 9, 2009.)

1547-5271/$ -see front matter doi:10.1016/j.hrthm.2009.11.012

Methods

Database

We constructed a database for analyzing resting 12-lead ECGs recorded in our hospital, which is associated with the Shiga University of Medical Science. A total of 102,065 patients (49,286 females and 52,779 males) who had undergone ECG recordings between January 1983 and October 2008 were collected in our database, and a total of 308,391 ECG recordings were performed during this period. Twelve leads were simultaneously acquired. The 12-lead ECG was recorded for 10 seconds at a sweep speed of 25 mm/s and calibrated to 1 mV/cm in the standard leads. ECG signals were recorded at an interval of 2 ms (i.e., 500 Hz). Digital data were stored on a computer server with 12-bit resolution. From the database, patients who fulfilled ECG criteria of LA overload were chosen using the analysis software MUSE7.1 (GE Marquette Medical Systems, Inc., Milwaukee, WI, USA). Computer-processed ECGs defined LA overload criteria as follows. (1) ECGs displaying biphasic P wave in lead V_1 were chosen. (2) The P wave was divided into the positively deflected portion in the initial P wave and the negatively deflected portion in the terminal P wave. (3) The terminal P wave in lead V_1 with duration $\geq$0.06 second and amplitude ≤ -0.2 mV (i.e., P terminal force $\geq$0.12) was considered as meeting LA overload criteria in this study (Figure 1).

Study participants

From our database, 78 participants who had marked LA overload were selected and assessed for the development of AF. A control group of 234 participants who did not have LA overload also was selected (1:3 matching). Individual matching was performed accounting for confounders (age, gender, date when ECG was taken), and when control candidates numbered more than three, the three controls were chosen randomly from among the candidates. The research protocol was approved by the Ethical Committee of Shiga University of Medical Science (19–75).

Digital analysis of ECG

The MUSE7.1 software detected identical P waves using a template matching technique. A point that had an area $\geq$160 μV/ms from the baseline level was considered to be P-wave onset, and a point that had an area $\leq$160 μV/ms from the baseline level was considered to be P-wave offset. The duration, amplitude, and area of total P wave, initial P wave, and terminal P wave in lead V_1 were measured using matrix parameters available in MUSE7.1. P-wave area was constructed by integrating the duration and amplitude. Duration $\times$ amplitude of P-wave initial and terminal portions in lead V_1 were calculated as force values. These variables were composed using the average value of the P wave during 10 seconds of recording time. Because all measurements of 12-lead ECGs were performed digitally using MUSE7.1, neither intraobserver nor interobserver variability occurred in this study.

Statistical analysis

The occurrence of AF was set as an endpoint, and the prognostic factors for developing AF were explored in the analysis. Patients whose ECG exhibited AF during the follow-up period (AF group) were compared with patients who did not (non-AF group). The follow-up period was defined as the interval between the first day when an ECG with LA overload was recorded and the first day when an ECG displaying AF was recorded in the AF group, or the interval between the first day when an ECG with LA overload was recorded and the latest day when an ECG was recorded in the non-AF group. The occurrence of death from any cause during the follow-up period was assessed by mail questionnaire. Written informed consent was obtained from all patients. Data are given as mean $\pm$ SD or percentage, and group comparisons were made using t-test or Mann-Whitney test, as appropriate. Categorical variables were compared using the Fisher exact test. Comparison of AF occur-

Figure 1 **A:** Twelve-lead ECG showing typical pattern of left atrial overload in lead V_1. *Red arrow* indicates P-wave negative terminal portion in lead V_1. *Asterisks* indicate P waves with identical morphology detected by template matching. **B:** Magnified ECG trace of lead V_1. *Blue arrow* indicates P-wave onset. *Green arrow* indicates P-wave offset.

rence between patients with LA overload and control patients was performed by logistic regression analysis and reported as odds ratio with 95% confidence interval (CI). Kaplan-Meier curves were used for determining the difference between two groups, and log rank test was used for examining the difference. Cox proportional hazard regression was used to estimate multivariate adjusted hazard ratios accounting for confounders (age, sex, cause of heart disease, ECG variables of P wave). All statistical tests were two-tailed, and $P < .05$ was considered significant.

Results

Atrial fibrillation

A total of 78 patients (mean age 52 ± 19 years) who fulfilled ECG criteria of marked LA overload were selected from our database using the GE Marquette 12SL ECG analysis program and enrolled for ECG analysis in this study. Of these patients, 15 (19%) developed AF (AF group), whereas 63 did not present AF (non-AF group). The control group consisted of 234 patients who were well matched for age (52 ± 19 years) and gender (78 women and 156 men; Table 1). AF developed in 3 (1.3%)of 234 control patients. The incidence of AF in patients with marked LA overload was 15-fold higher than that in control patients ($P < .001$). The odds ratio for occurrence of AF in patients with LA overload compared with control patients was 18.3 (95% CI 5.15–65.3). The mean follow-up period of the control patients was significantly longer than that of the patients with LA overload (78 ± 73 months vs 43 ± 52 months; $P < .001$). Kaplan-Meier survival analysis is shown in Figure 2. The AF-free event rate was significantly higher ($P < .001$) in patients with LA overload than in control patients (hazard ratio 24.5, 95% CI 7.94–107.3).

Characteristics of the patients

The clinical characteristics of patients in the AF and non-AF groups are listed in Table 2. The mean follow-up period of the AF group and non-AF group averaged 45 ± 61 months and 43 ± 50 months, respectively ($P = .93$). No significant difference with regard to age and sex was disclosed between the AF and non-AF groups. The average age at ECG documentation of AF was 59 ± 13 years. In the AF group, 14 (93%) of 15 patients had structural heart diseases such as hypertension, myocardial infarction, valvular heart diseases, and nonischemic cardiomyopathy. In contrast, structural heart disease was present in 46 (73%) of 63 patients in the non-AF group ($P = .081$). The presence of hypertension was more frequent in the AF group than in the non-AF

Table 1 Comparison of characteristics of control patients and patients with left atrial overload

	Control	Left atrial overload
No. of patients	214	78
Age (years)	52.4 ± 19.3	52.4 ± 19.3
Male [n (%)]	156 (66.7)	52 (66.7)
Follow-up period (months)	78.0 ± 72.9*	43.3 ± 52.0

Values are given as mean ± SD unless otherwise indicated.
*$P < .001$ vs patients with left atrial overload.

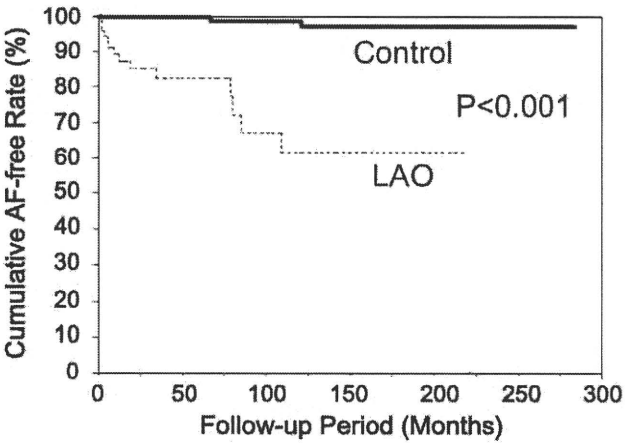

Figure 2 Kaplan-Meier estimates of atrial fibrillation (AF)-free event rate in patients with left atrial overload (LAO) and control patients. The difference between the two groups was significant ($P < .001$ by log rank test).

Table 2 Characteristics of the patients

Characteristic	AF group (n = 15)	Non-AF group (n = 63)	P value
Age (years)	55.8 ± 14.7	51.6 ± 20.3	.22
Gender (male/female)	10/5	42/21	1
Structural heart disease	14 (93)	46 (73)	.063
Hypertension	9 (60)	20 (31)	.045
Valvular heart disease	7 (47)	16 (25)	.12
Myocardial infarction	0 (0)	8 (13)	.06
Nonischemic cardiomyopathy	3 (20)	15 (24)	.66
Hypertrophic cardiomyopathy	3 (20)	7 (11)	.38
Dilated cardiomyopathy	0 (0)	8 (13)	.06
NYHA functional class I/II/III/IV	13/2/0/0	30/28/5/0	.80
Left ventricular ejection fraction (%)	63.2 ± 9.89	54.0 ± 18.5	.04
Antiarrhythmic drug			
Class IA	6	2	.01
Class IC	1	1	.32
Class III	1	0	.07
Diuretic	5	21	.70
Beta blocker	5	9	.32
Calcium antagonist	2	14	.44
Angiotensin II receptor blockade	1	2	.55
Angiotensin-converting enzyme inhibitor	3	8	.48
Nitrate	3	11	.81
Digitalis	5	15	.37
Oral anticoagulant	5	11	.14
Aspirin	3	5	.20

Values are given number, number (%), or mean ± SD.
AF = atrial fibrillation; NYHA = New York Heart Association.

group (odds ratio 3.2, 95% CI 1.01–10.3; $P = .04$), but other structural heart diseases showed no significant difference between the two cohort groups. Of note, the prevalence of both hypertension and valvular heart disease was significantly higher in the AF group (4/15 [26.7%]) than in the non-AF group (3/63 [4.8%]; odds ratio 7.3, 95% CI 1.4–37.1; $P = .018$).

Characteristics of ECG

ECG characteristics are listed in Table 3. No significant difference with regard to heart rate and frontal plane P-wave axis was seen between the AF and non-AF groups. The total duration of P wave in lead V_1 was significantly longer in the AF group than in the non-AF group. In contrast, the total amplitude (amplitude from top to bottom level) of the P wave in lead V_1 was not significant between the two groups.

For the two cohorts, we first evaluated the P-wave terminal portion in lead V_1, which was assigned as a marker for choosing patients from the database in the study. Table 4 (top) lists measurements of the P-wave terminal portion in lead V_1. The area of the P-wave terminal portion did not differ between the AF and non-AF groups. Neither the duration nor the amplitude of the P-wave terminal portion was different between the AF and non-AF groups. The same was true for the P-wave terminal force between the two groups. Because no significant difference in P-wave terminal portion in lead V_1 was observed between the AF and non-AF groups, we then estimated the initial portion of P wave in lead V_1. Table 4 (bottom) lists measurements of the P-wave initial portion in lead V_1. The area of the P-wave initial portion was significantly larger in the AF group than in the non-AF group. The duration of the P-wave initial portion was significantly longer in the AF group than in the non-AF group, and the amplitude of the P-wave initial portion was significantly higher in the AF group than in the non-AF group. Therefore, the P-wave initial force was significantly greater in the AF group than in the non-AF group.

AF development

Based on the significant association of the P-wave initial portion in lead V_1 with AF development, the AF-free event rate was estimated according to the area of P-wave initial portion. Using receiver operating characteristic analysis, the sensitivity and specificity of P-wave initial portion in response to developing AF were maximized by the area of P-wave initial portion of 65 (relative risk 4.0, 95% CI 1.2–13.1). Kaplan-Meier life-table analysis is shown in Figure 3. The area of the P-wave initial portion was associated with a significant difference of AF-free event rate between patients with area of P-wave initial portion ≥65 (n = 39) and those with area of P-wave initial portion <65 (n = 39; hazard ratio 4.02, 95% CI 1.25–17.8; $P = .02$). The rate of use of Class I antiarrhythmic drugs was identical between patients with area of P-wave initial portion ≥65 and those with area of P-wave initial portion <65 (10% vs 8%; $P = .72$). Because age is an important factor affecting the development of AF, the AF-free event rate was compared between patients <65 years old (n = 55) and those ≥65 years (n = 23). No significant difference was seen with regard to age (hazard ratio age ≥65 years to age <65 years = 2.39, 95% CI 0.72–7.19; $P = .12$). The AF-free event rate between patients with and those without hypertension was compared because hypertension was more prevalent in the AF group than in the non-AF group, but the presence of hypertension did not significantly affect the development of AF (hazard ratio of presence to absence of hypertension = 1.4, 95% CI 0.4–4.4; $P = .54$). In addition, no significant gender difference was found with regard to the AF-free

Table 3 Characteristics of ECG

Measurement	AF group	Non-AF group	*P* value
Heart rate (bpm)	69.0 ± 22.4	84.1 ± 19.3	.99
P-wave axis (°)	60.5 ± 20.5	61.9 ± 14.3	.62
P wave (ms) in lead V_1			
Total duration (ms)	126.7 ± 14.8	115.8 ± 16.7	.012
Total amplitude (μV)	310.7 ± 15.8	302.9 ± 64.9	.33

Table 4 Measurements of P wave in lead V_1

Measurement	AF group	Non-AF group	*P* value
Terminal Portion			
Duration (ms)	84.5 ± 15.0	80.1 ± 12.5	.123
Amplitude (μV)	−216.7 ± 20.1	−234.0 ± 40.0	.108
Area (μV × ms)	468.2 ± 155.0	477.7 ± 139.5	.41
Terminal force (s × μV)	18,491 ± 5,149	18,779 ± 4,584	.42
Initial Portion			
Duration (ms)	42.2 ± 12.4	35.7 ± 10.1	.018
Amplitude (μV)	94.0 ± 39.9	68.8 ± 49.4	.035
Area (μV × ms)	114.6 ± 73.0	73.1 ± 59.3	.011
Initial force (s × μV)	4,346.7 ± 2,712	2,650.3 ± 2,375	.0089

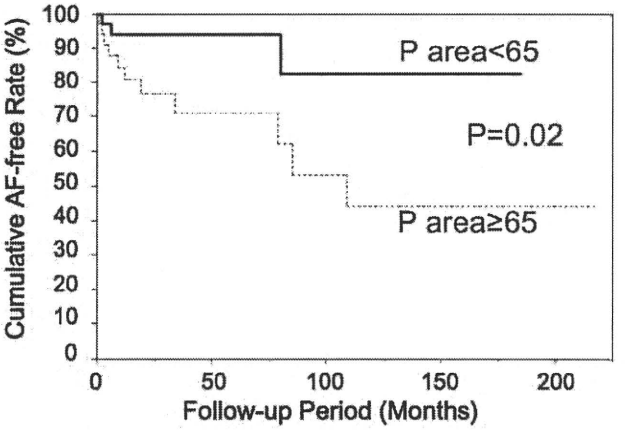

Figure 3 Kaplan-Meier estimates of atrial fibrillation (AF)-free event rate in patients with left atrial overload according to the area of P-wave initial portion in lead V_1. The AF-free event rate in patients with area of P-wave initial portion ≥65 μV × ms was significantly lower than in those with area of P-wave initial portion <65 μV × ms ($P = .02$).